Quadratic rational rotations of the torus and dual lattice maps

K. L. Kouptsov, J. H. Lowenstein and F. Vivaldi†

Dept. of Physics, New York University, 2 Washington Place, New York, NY 10003, USA
†School of Mathematical Sciences, Queen Mary, University of London, London E1 4NS, UK

Abstract

We develop a general formalism for computed-assisted proofs concerning the orbit structure of certain non ergodic piecewise affine maps of the torus, whose eigenvalues are roots of unity. For a specific class of maps, we prove that if the trace is a quadratic irrational (the simplest nontrivial case, comprising 8 maps), then the periodic orbits are organized into finitely many renormalizable families, with exponentially increasing period, plus a finite number of exceptional families. The proof is based on exact computations with algebraic numbers, where units play the role of scaling parameters. Exploiting a duality existing between these maps and lattice maps representing rounded-off planar rotations, we establish the global periodicity of the latter systems, for a set of orbits of full density.

1 Introduction

Discontinuous, piecewise affine maps appear in a variety of dynamical contexts, such as polygonal dual billiards [23, 15, 22], polygonal exchange transformations [16], the dynamics of digital filters [7, 8, 9, 25, 11, 4], the propagation of round-off errors in linear systems [19, 20, 21], and are of general interest in the theory of dynamical systems [3, 1, 13, 14, 18]. For an overview, see [1].

In this class of systems, the topology of the phase space is shaped by discontinuity rather than nonlinearity, resulting in strikingly complex behaviour from minimal ingredients. The theoretical development is fragmented, with relatively few general results and many studies of specific models, where the proofs tend to be burdened by cumbersome notation and tedious book-keeping, which are required to manipulate complex arrangements of simple geometrical objects.

A common set-up is that of a lattice $\mathbf{L} \in \mathcal{R}^n$ and an $n \times n$ matrix C that does not leave $\mathbf{L}$ invariant. One lets C act on some fundamental domain Ω for $\mathbf{L}$, reducing coordinates after each iteration. This action is discontinuous, and it depends not only on $\mathbf{L}$ and C, but also on the choice of the fundamental domain Ω. Of interest are invertible non-ergodic mappings, where the eigenvalues of C have unit modulus. These systems have zero metric entropy [12, 16, 1, 6].

In the present investigation, we consider a specific class of discontinuous affine maps of the torus, which are dual to invertible rounded-off rotations of the plane. Special cases of such torus maps have been studied in the literature [20, 21, 1, 18] (not necessarily with reference to this duality). The present work provides complete results for specific maps, and a general framework for the entire class, supported by a set of computer-based tools for analyzing the dynamics, both at the level of experiments and of rigorous computer-assisted proof.

The idea is to identify conditions under which the relevant geometry takes place in an algebraic number field, where exact computation becomes possible, limited only by storage and time constraints. The strategy is to discover theorems experimentally, and then use exact arithmetic and induction to prove them.

The torus maps studied here are constructed as follows. We fix two coprime integers p and q, and let

$$\xi = \exp(2\pi i\, p/q); \qquad \lambda = \xi + \xi^{-1} = 2\cos(2\pi\, p/q); \qquad \tau = \lambda^{-1}. \tag{1}$$

Then we introduce the matrix

$$C = \begin{pmatrix} \lambda & -1 \\ 1 & 0 \end{pmatrix}, \tag{2}$$

which is conjugate to a planar rotation by the angle $2\pi p/q$. The parameter λ is an *algebraic integer,* namely, the root of a polynomial with integer coefficients and unit leading coefficient (see Section 2). A minimal set of values of p/q for which this polynomial is *quadratic,* is given by

$$\frac{1}{5}, \frac{2}{5}, \frac{1}{8}, \frac{3}{8}, \frac{1}{10}, \frac{3}{10}, \frac{1}{12}, \frac{5}{12}. \tag{3}$$

This paper is concerned with the dynamics for these rotation numbers. Due to the quadratic equations satisfied by λ and τ, all relevant arithmetic involves numbers of the form $r + s\lambda$ with r and s rational — the quadratic field $\mathbf{Q}(\lambda)$ — and related sets, to be described in Section 2. Computation with algebraic numbers is exact, involving integers and the symbolic (as opposed to numerical) representation of λ and τ.

Next, given a non zero number κ (the *scale factor*), and a number ι with $-1 < \iota \leq 0$ (the *off-set*), we define a lattice $\mathbf{L}$ with fundamental domain Ω, as follows

$$\Omega = (\kappa I)^2, \qquad I = [\iota, \iota + 1), \qquad \mathbf{L} = (\kappa \mathbf{Z})^2 \qquad \kappa, \iota \in \mathbf{Q}(\lambda). \tag{4}$$

(The significance of the scale factor κ will be clear below.) To the triple $(C, \mathbf{L}, \Omega)$ we associate two dynamical systems:

$$\begin{array}{lll} \textit{torus map} & \Phi : \Omega \to \Omega & \zeta \mapsto (C \cdot \zeta - \mathbf{L}) \cap \Omega \\ \textit{lattice map} & \Psi : \mathbf{L} \to \mathbf{L} & z \mapsto (C \cdot z - \Omega) \cap \mathbf{L} \end{array} \tag{5}$$

These maps, whose action is sketched in figures 1 and 2, respectively, are well-defined, because Ω is a fundamental domain for $\mathbf{L}$. Furthermore, they are invertible, as a result of the particular form of the matrix C and of the domain Ω (C is a 'parquet matrix' for $\mathbf{L}$ and Ω, in the parlance of [1]). The lattice map describes rotation, subject to round-off, which, acts on the x-coordinate only via a rounding function R, defined by

$$R(x) = \kappa \left\lfloor \frac{x}{\kappa} - \iota \right\rfloor \in (x - \kappa I) \cap \kappa \mathbf{Z}. \tag{6}$$

We note some commonly used round-off schemes:

κ	ι	$R(x)$	
1	0	$\lfloor x \rfloor$	rounding down
-1	0	$\lceil x \rceil$	rounding up
1	$-1/2$	$\lfloor x + 1/2 \rfloor$	symmetric rounding, with $R(1/2) = 1$

A relation between a $(\mathbf{C}, \mathbf{L}, \Omega)$ lattice map Ψ and a $(\tilde{C}, \tilde{\mathbf{L}}, \tilde{\Omega})$ torus map Φ — invariably corresponding to different parameters — is established by embedding the lattice of the former into the fundamental domain of the latter [21]

$$\mathcal{E} : \mathbf{L} \to \tilde{\Omega} \qquad\qquad \Phi = \mathcal{E} \circ \Psi \circ \mathcal{E}^{-1}, \tag{7}$$

We call the systems *dual* of each other, if the embedding is uniform, and if the conjugate of Ψ on $\mathcal{E}(\mathbf{L})$ extends to a torus map of $\tilde{\Omega}$. In the present context, uniformity means that for every convex polyhedron $\Pi \subseteq \Omega$, the density of the set of lattice points z such that $\mathcal{E}(z) \in \Pi$ is equal to the normalized volume of Π. The process of embedding, whereby one constructs a dense and uniform image of a lattice in a compact set, is referred to as *localization,* due to its structural analogy with embedding algebraic number rings in the p-adics, used in related round-off maps [5, 24]. The dimensionality of the lattice map is usually greater than that of the round-off map. However, when the parameter λ in (2) is quadratic, the dimensionality is the same, and duality takes on a simple form, as detailed in the following

Theorem 1 *Let Ψ be the $(C, \mathbf{L}, \Omega)$ lattice map with parameters given by (1), (2) and (4). If λ is a root of a quadratic polynomial, then the mapping Ψ is dual to the torus map Φ, with scale factor $\kappa\tau$, the same off-set, and matrix*

$$\tilde{C} = \begin{pmatrix} \tilde{\lambda} & -1 \\ 1 & 0 \end{pmatrix}, \tag{8}$$

where $\tilde{\lambda}$ is the algebraic conjugate of λ.

With the choice $\kappa = 1$, the embedding (7) can be written explicitly as

$$\mathcal{E}(x, y) = (x - m_0\tau, y - m_1\tau) \qquad\qquad (x, y) \in \mathbf{Z}^2$$

where $m_0, m_1 \in \mathbf{Z}$ are uniquely determined by the condition $\mathcal{E}(x, y) \in (\tau I)^2$.

One verifies that for the maps under consideration, the two sides of the square Ω are lines of discontinuity for both Φ and its inverse. Let W_0 be the union of those sides. The *discontinuity set* of Φ is defined as

$$W = \bigcup_{t=-\infty}^{\infty} \Phi^t(W_0). \tag{9}$$

The set W, which mimics the web of intersecting separatrices in nonlinear Hamiltonian systems, is portrayed in Figure 3 for the case $p/q = 5/12$. The complementary set $\Pi = \Omega \setminus \bar{W}$ is a (possibly empty) collection of countably many convex polygons Π_i, with at most $2q$ sides.

In Ref. [19], a complete dynamical analysis of the round-off map Ψ is given for $p/q = 1/5$ ($\lambda = (\sqrt{5} - 1)/2$), and $b = 0$ (rounding down to the nearest integer, i.e., floor function). By exploiting the duality with a torus map, it is proven that all orbits are periodic, and fall into two scaling families. For each period, there are infinitely many congruent orbits, distributed quasiperiodically and with finite density over the lattice $\mathbf{Z}^2$. Their dual orbits (their image under the mapping $\mathcal{E}$) in the torus map are densely and uniformly distributed among the polygons Π_i in $\tilde{\Omega}$, in such a way that their density in $\mathbf{L}$ becomes the area of these polygons. As one progresses from one level of the scaling sequence to the next, the period scales asymptotically by a factor 4, while the area of the dual polygon is reduced exactly by λ^2.

To generalize the analysis of [19] for $p/q = 1/5$ to all quadratic λ, we must deal effectively with a considerably higher level of complexity. For example, for $p/q = 5/12$ we find six exceptional polygons which do not scale, while the shortest period of all the orbits in one of the two scaling sequences is greater than 10000. Here exact arithmetic and computer-assistance become essential. One of the principal goals of the present work is to prove rigorously the existence and completeness of scaling sequences of periodic orbits in the full set of torus/round-off maps for which λ is a quadratic integer and the interval I in (4) is $[0, 1)$ (rounding down convention). We formulate this as our second main theorem (see Sections 2 and 4, for relevant definitions)

Theorem 2 *For the 8 quadratic rounding-down models ($\iota = 0, \kappa = 1$, and rotation numbers (3)), the domain Ω can be partitioned, apart from a set of measure zero, a finite number of infinite scaling sequences of periodic domains, plus a finite number of exceptional open periodic domains, which do not scale. The scaling constant of each sequence is a unit of positive norm in the ring of integers of $\mathbf{Q}(\lambda)$.*

Theorem 2 is supplemented by the following table, where we list, for each rotation number p/q, the number $\#E$ of exceptional periodic domains of positive measure, the number $\#S$ of scaling families of periodic domains, and the parameters associated to such families, namely the scaling constant ω and the limit point ζ^*. The scaling constant is expressed in terms of the fundamental unit η of the relevant field, as detailed in Table II (Section 2).

TABLE I

ORBIT CLASSES AND SCALING PARAMETERS

p/q	$\#E$	$\#S$	ω	η^k	ζ^*
1/5	3	2	$2-\tau$	η^{-2}	$(0,0)$
2/5	1	2	$1+\tau$	η^{-2}	$(0,0)$
1/8	3	2	$3-4\tau$	η^{-2}	(τ,τ)
3/8	0	2	$3+4\tau$	η^{-2}	$(0,\tau)$
1/10	4	2	$1-\tau$	η^{-2}	(τ,τ)
3/10	0	2	$2+\tau$	η^{-2}	$(0,\tau)$
1/12	8	3	$7-12\tau$	η^{-2}	(τ,τ)
5/12	6	1	$2+3\tau$	η^{-1}	(τ,τ)
		1	$2+3\tau$	η^{-1}	$(41+72\tau, 41+72\tau)$

Theorems 1 and 2 imply the global periodicity of the corresponding dual lattice map Ψ, which we define here explicitly

Corollary 1.1 *Let $\Psi : \mathbf{Z}^2 \to \mathbf{Z}^2$ be given by*

$$(x, y) \mapsto (\lfloor \lambda x \rfloor - y, x) \qquad\qquad \lambda = 2\cos(2\pi p/q)$$

where $\lfloor\cdot\rfloor$ is the floor function. If λ is a quadratic integer, then all orbits of Ψ are periodic, except, possibly, a set of zero density.

The possible exclusion of a set of zero density is connected to the discontinuity set of the dual toral map. The orbits on this set, may or may not be periodic [1, 18], and are not necessarily relevant to the map on the dual lattice $\mathbf{L}$, since they may not belong to its local image $\mathcal{E}(\mathbf{L})$. The singular orbits form convex polygons of lower dimension, which can reduce to points.

We have carried out the analysis of these orbits in some cases. For $p/q = 1/5$, the boundary of one of the two scaling families can be glued to its interior, with which it shares the itinerary in phase space. The discontinuity set contains no new topological information, and has a dual image [19]. By contrast, for $p/q = 1/8$, we find that the measure-bearing orbits (open octagons) are topologically distinct from the orbits on their boundary, with a further differentiation between edges and vertices. Again, the discontinuity set has a dual counterpart on the lattice: the edges correspond to infinite families of periodic orbits aligned along one-dimensional sublattices of $\mathbf{L}$; the vertices correspond to scaling sequences of orbits surrounding the origin. Necessarily, all these orbits have zero density. For $p/q = 3/8$, we find a scaling sequence of periodic domains, as well as a Cantor set of aperiodic orbits By modifying the lattice map, and exploiting duality, we were able to construct a lattice map with unbounded orbits. See propositions 6.1–6.3 of section 6 for precise statements.

Finally, there is the *residual set*, namely the complement of the discontinuity set in its closure, which may have a non-trivial Hausdorff dimension. From Theorem 2 one has that in the quadratic case, the multifractal spectrum of the residual set has only finitely many scaling constants, associated to the orbits classes. Their dimension is given by the logarithmic ratio of temporal and spatial scaling factors. A study of the dynamics and multifractal properties of the residual set, although of considerable interest in connection with the transport properties of the dual round-off model [20], is beyond the scope of the present investigation. We only remark that the hierarchical organization of the residual set disappears in the cubic case [21].

This article is organized as follows. In Section 2, after reviewing the necessary arithmetical background, we prove Theorem 1. In Section 3, we introduce the geometrical and dynamical concepts that underpin the definition of scaling sequences and domains, given in Section 4. The computer-assisted proof of Theorem 2 is given in Section 5, while Section 6 deals with a complete characterization of the discontinuity set in two important examples. The second of these completes the analysis of a torus map studied in [1], where the discontinuity set features both periodic orbits, as well as a Cantor set or aperiodic ones. Exploiting this result and duality, we construct a round-off model with escape orbits. In Section 7 we offer concluding remarks. The structure of the computer-assistant and the procedures involved is described in Appendix A; a sample proof for the case $p/q = 1/5$ is presented in Appendix B. The bulk of the data required for the proofs is tabulated in Appendix C; details of the computer-assisted proof are available in the form of Mathematica notebooks at the web site `http://poincare.physics.nyu.edu/ jhl2/ComputerAssistant/`.

2 Arithmetical preliminaries and duality

In this section we describe the arithmetical environment relevant to the dynamics of quadratic torus and lattice maps. The reader requiring background references, may consult [2] and [10].

The parameter λ in equation (1) is required to be quadratic. Accordingly, the associated root of unity ξ is a root of a polynomial of degree four, the qth cyclotomic polynomial $H_q(x)$. Because the degree of $H_q(x)$ is $\phi(q)$ (the Euler's function at q, i.e., the number of positive integers not exceeding q and coprime to it), the set $\phi^{-1}(4)$ provides the denominators of the rationals listed in (3).

From the identities[1]

$$(i) \qquad \sum_{\substack{1\leq p<q\\ \gcd(p,q)=1}} e^{2\pi\, ip/q} = \mu(q); \qquad\qquad (ii) \qquad x^{\phi(q)} H_q(1/x) = H_q(x) \qquad (10)$$

[1] (i) is Ramanujan's identity ([2], chapter 8); (ii) follows from the fact that if ξ is a root of $H_q(x)$, so is ξ^{-1}.

where μ is the Möbius function ($\mu(1) = 1$; $\mu(x) = 0$ if x has a square divisor; $\mu(x) = (-1)^k$ if x is square-free and has k prime divisors), it follows that

$$H_q(x) = x^4 - \mu(q)x^3 + h(q)x^2 - \mu(q)x + 1.$$

Using ($10i$), one can show that

$$h(q) = \begin{cases} \mu(q)(\mu(q)-1)/2 & q \text{ odd} \\ \mu(q)(\mu(q)+1)/2 & 4 \not| q \\ -\mu(q/2) & 4 \mid q \end{cases} \qquad \phi(q) \geq 4.$$

Expressing $H_q(x)x^{-2}$ as a function of $\lambda = x + x^{-1}$, we obtain the quadratic polynomial $G_q(x)$ with roots λ and its conjugate $\tilde{\lambda}$

$$G_q(x) = x^2 - \mu(q)x + h(q) - 2 = 0 \tag{11}$$

and the corresponding polynomial $L_q(x)$ for τ

$$L_q(x) = x^2 G_q(x^{-1}). \tag{12}$$

From equations (1) and (11) we obtain

$$\tilde{\lambda} = \mu(q) - \lambda = (h(q) - 2)\tau. \tag{13}$$

The underlying coordinate field is the quadratic field $\mathbf{Q}(\lambda)$ and its ring of integers $\mathbf{Z}[\lambda]$

$$\mathbf{Q}(\lambda) = \{r + s\lambda\} \quad r, s \in \mathbf{Q}; \qquad \mathbf{Z}[\lambda] = \{m + n\lambda\} \quad m, n \in \mathbf{Z}.$$

Most of the computation will take place in a prominent subsets of $\mathbf{Q}(\lambda)$, namely

$$\mathcal{M} = \kappa\mathbf{Z}[\lambda] + \kappa\iota\mathbf{Z}[\lambda] \tag{14}$$

which is the sum of two copies of $\mathbf{Z}[\lambda]$, multiplied by the parameters defining $\mathbf{L}$ and Ω (cf. equation (4)). Unlike $\mathbf{Z}[\lambda]$, $\mathcal{M}$ is not closed under multiplication, in general; however, $\mathcal{M}$ enjoys the closure property $\mathbf{Z}[\lambda] \times \mathcal{M} = \mathcal{M}$, which makes it into a $\mathbf{Z}[\lambda]$-module, i.e., a vector space where the 'scalars' are the elements of $\mathbf{Z}[\lambda]$.

The module $\mathcal{M}$ appears in the recursive construction of the discontinuity set. This is because $\mathcal{M}^2$ is C-invariant, and the lattice translations required to iterate Φ are in $\mathcal{M}^2$. We will show (section 3) that all convex components of the discontinuity set, and of its complement, are defined by inequalities over $\mathcal{M}$. Furthermore there is an integer a such that the Φ-invariant set

$$\Omega \cap \left(\frac{1}{a}\mathcal{M}\right)^2 \tag{15}$$

contains all vertices of all components of the discontinuity set. It follows that the measure of these polygons also belongs to a fractional module of $\mathcal{M}$.

The module $\mathcal{M}$ has an integral basis. For our purpose, it suffices to consider the case $\mathcal{M} = \tau\mathbf{Z}[\lambda]$, corresponding to scale factor $\kappa = n\tau$, and off-set $\iota = -m/n$, with m and n coprime integers. In this case we have the explicit representation

$$\mathcal{M} = \tau\mathbf{Z}[\lambda] = \{m + n\tau\} \qquad m, n \in \mathbf{Z}. \tag{16}$$

We list in Table II the relevant arithmetical data. We have introduced the quadratic form $Q(x, y)$, which represents the *norm* $N(\zeta) = \zeta\tilde{\zeta}$ of ζ with respect to the basis $[1, \lambda]$; that is, if $\zeta = x + y\lambda$, then $Q(x, y) = N(\zeta)$. The minimal polynomials $G(x)$ and $L(x)$ of λ and τ, respectively (equations (11) and (12)), are expressed in terms of $Q(x,y)$ as follows

$$G(x) = Q(-x,1) \qquad\qquad L(x) = x^2\, Q(-1/x,1). \tag{17}$$

The scaling constants appearing in Theorem 2 are units, that is, elements of $\mathbf{Z}[\lambda]$ whose norm is ± 1. The fundamental unit η is the smallest unit greater than one: it has the property that $\pm\eta^k$, $k \in \mathbf{Z}$, exhausts all units in $\mathbf{Z}[\lambda]$. The columns in Table II are ordered from left to right according to increasing specialization. Thus the fundamental unit η depends only on the field discriminant $d = (\tilde{\lambda}-\lambda)^2$, and for a given discriminant, the value of μ depends only on the denominator q of the rotation number, etc.

Table II

ARITHMETICAL PARAMETERS

d	η	$N(\eta)$	q	$\mu(q)$	$Q(x,y)$	p	λ
5	$(1+\sqrt{5})/2$	-1	5	-1	x^2-xy-y^2	1	$(-1+\sqrt{5})/2$
						2	$(-1-\sqrt{5})/2$
			10	$+1$	x^2+xy-y^2	1	$(1+\sqrt{5})/2$
						3	$(1-\sqrt{5})/2$
8	$1+\sqrt{2}$	-1	8	0	x^2-2y^2	1	$\sqrt{2}$
						3	$-\sqrt{2}$
12	$2+\sqrt{3}$	$+1$	12	0	x^2-3y^2	1	$\sqrt{3}$
						5	$-\sqrt{3}$

2.1 Proof of Theorem 1

Without loss of generality, we choose the scale factor of the lattice mapping Ψ to be $\kappa = 1$ in (4), corresponding to the lattice $\mathbf{L} = \mathbf{Z}^2$. In vector notation, we can write Ψ as follows

$$\Psi\begin{pmatrix} x \\ y \end{pmatrix} = \begin{pmatrix} R(\lambda x) - y \\ x \end{pmatrix} \qquad\qquad x,\, y \in \mathbf{Z} \tag{18}$$

where R is the one-dimensional round-off function defined in (6).

We embed $\mathbf{Z}^2$ into the domain $\tilde{\Omega}$ with scale factor $\kappa = \tau$ and the same off-set, as follows

$$\mathcal{E}\begin{pmatrix} x \\ y \end{pmatrix} = \begin{pmatrix} x - R(\lambda x)\tau \\ y - R(\lambda y)\tau \end{pmatrix}. \tag{19}$$

Let us now calculate the action of the torus map $\tilde{C}$ on $\zeta \in \tilde{\Omega} \cap \mathcal{E}(\mathbf{Z}^2)$:

$$\begin{aligned} \tilde{C}\cdot\zeta &= \begin{pmatrix} \mu(q)-\lambda & -1 \\ 1 & 0 \end{pmatrix}\begin{pmatrix} x - R(\lambda x)\tau \\ y - R(\lambda y)\tau \end{pmatrix} \\ &= \begin{pmatrix} R(\lambda x) - y + \tau\left[(h(q)-2)x - \mu(q)R(\lambda x) + R(\lambda y)\right] \\ x - R(\lambda x)\tau \end{pmatrix} \end{aligned}$$

where we have used identity (13). Making a suitable translation by the lattice $\tilde{\mathbf{L}} = \tau\mathbf{Z}^2$, we get

$$\Phi(\zeta) = \begin{pmatrix} R(\lambda x) - y - R(\lambda(R(\lambda x)-y))\tau \\ x - R(\lambda x)\tau \end{pmatrix} = \mathcal{E}(\Psi(\mathcal{E}^{-1}(\zeta))),$$

which is seen to extend to the $(\tilde{\Omega},\, \tilde{\mathbf{L}},\, \tilde{C})$ torus map.

Multiplying both sides of equation (19) by λ, we see that, on each coordinate, $\mathcal{E}$ acts as a scaled version of the map that sends x to the fractional part of λx. Because λ is irrational, the density of points that map on any finite disjoint union of intervals is equal to the measure of these intervals, from Weyl's theorem ([17], theorem 445). The correspondence between density and measure extends to the pre-images of two dimensional polygons, since the latter have piecewise smooth boundary. (See also [20], section 2.) $\square$

A duality for lattice maps of the type (18) with arbitrary q, was established in [21]. In this case, the lattice is embedded into a torus of dimension $\phi(q)-2$. For the quadratic cases, the matrix analogous to (8) is

$$\begin{pmatrix} 0 & 1 \\ -1 & \mu(q)-\lambda \end{pmatrix} \tag{20}$$

which is conjugate to $\tilde{C}$ via interchange of coordinates. The embedding is given by

$$\begin{pmatrix} x \\ y \end{pmatrix} \mapsto \begin{pmatrix} x - m_0\tau \\ m_0 - y - m_1\tau \end{pmatrix},$$

with

$$m_0 = R(\lambda x), \qquad m_1 = R(\lambda(m_0 - y)).$$

In the present work, we have performed some calculations using the representation (20), to make use of software already developed.

3 Domains

3.1 Definitions and notation

For a $(C, \mathbf{L}, \Omega)$ torus map of the type considered here, there are only q allowed orientations for the lines of the discontinuity set, whose equations are written as

$$u \cdot \zeta = b \tag{21}$$

where $u \in \mathbf{Z}[\lambda]^2$ is one of the q vectors

$$u^{(i)} = (\tilde{C}')^i \cdot \begin{pmatrix} 1 \\ 0 \end{pmatrix} \qquad i = 0, \ldots, q-1 \tag{22}$$

with a prime denoting the transpose. Note that for q even, $(\tilde{C}')^{q/2}$ is just a reflection, so that each allowed direction has an oppositely directed partner.

Since the polygons Π_i are convex and bounded by lines of the discontinuity set, the restriction on line directions leads to a simple notation for specifying and manipulating them. We define a *domain* to be a non-empty planar convex set specified by B bounds of the form

$$\begin{array}{llll} u^{(j)} \cdot \zeta \geq b_{j-} & \text{or} & u^{(j)} \cdot \zeta < b_{j+}, & \lambda > 0 \\ u^{(j)} \cdot \zeta > b_{j-} & \text{or} & u^{(j)} \cdot \zeta \leq b_{j+}, & \lambda < 0 \end{array} \qquad j = 0, \ldots, B-1 \tag{23}$$

where $b_{j\pm} \in \mathcal{M}$, and $\zeta = (\zeta_0, \zeta_1)$ is a point on the plane. Domains need not be a two-dimensional polygons; they can be lines (for even q), line segments, and points, which will help dealing with objects of different dimension with a unified formalism. For example, for $q = 8$, the inequalities $u^{(0)} \cdot \zeta \geq 1$, $u^{(4)} \cdot \zeta \geq -1$ specify the line $\zeta_0 = 1$.

The inequalities (23) defining a domain will be written more compactly as

$$s_j u^{(m_j)} \cdot \zeta < s_j b_j \quad \text{or} \quad s_j u^{(m_j)} \cdot \zeta \le s_j b_j, \qquad j = 0, \ldots, B-1 \tag{24}$$

with

$$s_j \in \{-1, 1\}, \qquad m_j \in \{0, \ldots, q-1\}, \qquad b_j \in \mathcal{M}.$$

We use the notation $D(\mathbf{m}, \mathbf{s}, \mathbf{b})$ for such a domain, where $\mathbf{m}$, $\mathbf{s}$, and $\mathbf{b}$ are B-dimensional vectors. To specify individual inequalities, we will use the shorthand notation $(m_j^{s_j}, b_j)$ to denote the relation (24).

3.2 Vertices and area

The lines perpendicular to $u^{(m_j)}$ and $u^{(m_k)}$ intersect if $m_j \neq m_k, m_k \pm q/2$, and the coordinates of the intersection ζ are determined by solving the linear equations

$$u^{(m_j)} \cdot \zeta = b_j, \qquad u^{(m_k)} \cdot \zeta = b_k.$$

The intersection point ζ, is a *vertex* of the domain if it lies on its boundary, i.e., it satisfies all of the domain inequalities with $<$ replaced by $\le$. We have that $\zeta \in (\mathcal{M}/a)^2$, where a is the least common multiple of the determinants $\left| u^{(j)}\, u^{(k)} \right|$.

A bounded domain is either a point (1 vertex), a line segment (2 vertices), or a polygon (more than 2 vertices). The simplest way of verifying that a set satisfying inequalities of the type (24) is nonempty is to verify the existence of one or more vertices. To produce an interior point in a domain with more than one vertex, we compute the centroid (mean of the vertices).

The closure $\bar{D}$ of a domain D (defined by (23), with all $<$ replaced by $\le$) is a set (not necessarily a domain) containing all vertices of D and of any sub-domain of D. To check whether a domain D' is a sub-domain of D, one verifies that the vertices of D' are in $\bar{D}$, but that is not always conclusive: one included edge of D' ($\le$ inequality) might not belong D ($<$ inequality), even though it does belong to $\bar{D}$. It is sufficient to check for the presence of the offending $<$ inequality among the defining relations of D. For example, if q is even and D' is a polygon with an included edge of type $(m_j^{s_j}, b_j)$, then one would look for an edge of D of type $((m_j + q/2)^{-s_j}, -b_j)$.

The *area* $\mathcal{A}(D)$ of a domain D with $N > 2$ vertices is computed by triangulation. Specifically, we first find the vertices of D and arrange them in cyclic order. The are of the triangle with vertices V_0, V_i, V_{i+1} is one-half the magnitude of the vector product of $V_i - V_0$ with $V_{i+1} - V_0$. Summing over i gives the area as an algebraic number in $\mathbf{Q}(\lambda)$.

3.3 Geometric transformations

We define (frame-dependent) operators which rotate, translate, and rescale domains.

The (generalized) *rotation* of a domain is defined as

$$\mathcal{R}\, D(\mathbf{m}, \mathbf{s}, \mathbf{b}) = D(\mathbf{m}', \mathbf{s}, \mathbf{b}), \tag{25}$$

where

$$m_j' \in \{0, \ldots, q-1\}, \qquad m_j' \equiv m_j - 1, \qquad j = 0, \ldots, B-1.$$

It is easy to verify that the right hand side of (25) is the domain obtained by applying the linear transformation with matrix $\tilde{C}$ to the boundary lines of $D(\mathbf{m}, \mathbf{s}, \mathbf{b})$.

For $\delta \in \mathcal{M}^2$, the *translation* of a domain by δ is defined by

$$\mathcal{T}_\delta D(\mathbf{m}, \mathbf{s}, \mathbf{b}) = D(\mathbf{m}, \mathbf{s}, \mathbf{b}'), \tag{26}$$

where

$$b'_j = b_j + u^{(m_j)} \cdot \delta \in \mathcal{M}. \tag{27}$$

One readily proves that the right-hand side of (26) is the domain obtained by translating $D(\mathbf{m}, \mathbf{s}, \mathbf{b})$ by the vector δ.

Finally, for any positive $\omega \in \mathbf{Z}[\lambda]$, we define the *rescaling* of a domain by

$$\mathcal{S}_\omega D(\mathbf{m}, \mathbf{s}, \mathbf{b}) = D(\mathbf{m}, \mathbf{s}, \omega\mathbf{b}). \tag{28}$$

It is easy to show that the right-hand side of (28) is the domain obtained from $D(\mathbf{m}, \mathbf{s}, \mathbf{b})$ by rescaling all coordinates by a factor ω. Note that $\omega \in \mathbf{Z}[\lambda]$, $b \in \mathcal{M}$ implies $\omega b \in \mathcal{M}$ (cf. comments following equation (14)).

For $\omega \in \mathbf{Z}[\lambda]$ and $\delta \in \mathcal{M}^2$, one verifies, from the above definitions, the commutation formulae for domain operators

$$\mathcal{R} \circ \mathcal{S}_\omega = \mathcal{S}_\omega \circ \mathcal{R}, \qquad \mathcal{T}_{\omega\delta} \circ \mathcal{S}_\omega = \mathcal{S}_\omega \circ \mathcal{T}_\delta. \tag{29}$$

Furthermore, for all domains D_1 and D_2, and $\omega \in \mathbf{Z}[\lambda]$, we have

$$D_1 \subset D_2 \iff \mathcal{S}_\omega D_1 \subset \mathcal{S}_\omega D_2$$

and the scaling of areas

$$\mathcal{A}(\mathcal{S}_\omega D_1) = \omega^2 \mathcal{A}(D_1). \tag{30}$$

The action of a torus map Φ amounts to a generalized rotation followed by a lattice translation. The set Ω — itself a domain — is partitioned into sub-domains Ω_j, by taking a single pre-image of the discontinuity set W_0. This partition will be referred to as the *generating partition.* On each sub-domain Ω_j, the action of Φ, is expressed in terms of the domain operators defined above as follows

$$\Phi(\Omega_j) = \mathcal{T}_{\delta_j^\Omega} \circ \mathcal{R}\Omega_j, \qquad \delta_j^\Omega = (0, -j\tau), \tag{31}$$

where $\delta_j^\Omega \in \mathcal{M}^2$ is determined uniquely by the condition $\Phi(\Omega_j) \subset \Omega$. It is clear that for a given map, δ_j^Ω can assume only finitely many values. The bounds defining the elements of the generating partition belong to the module $\mathcal{M}$, and remain in $\mathcal{M}$ under the action of domain operators. Hence the discontinuity set is described entirely by algebraic numbers in $\mathcal{M}$.

Our discussion of scaling in the next section will involve a shift of origin, from $(0,0)$ to some point $\zeta_* \in \mathcal{M}^2$. To give frame-independent meaning to the dynamical map Φ, we represent it as $\mathcal{T}_\delta \circ \mathcal{R}$, with

$$\delta = \delta_0 + (\mathcal{R} - \mathbf{1})\zeta_*,$$

in the coordinates relative to the point ζ_*.

In later sections, we will continue to use the notation $D(\mathbf{m}, \mathbf{s}, \mathbf{b})$ to specify domain boundaries in a translated frame of reference. It is easy to see that, when the origin is shifted from $(0,0)$ to ζ_*, the bound b_j is replaced by $b_j - u^{(j)} \cdot \zeta_*$, with $\mathbf{m}$ and $\mathbf{s}$ unchanged.

4 Return maps and scaling domains

We introduce the concepts of *return map* and *scaling domain*, which are central to our proof of Theorem 2.

Def. (*return map and return time*) Let D be a domain, partitioned into sub-domains D_j, each contained in some Ω_i, with the property that for each j, there exists a positive integer t_j — the *return time* for D_j — such that

$$\rho_j(D_j) \stackrel{\text{def}}{=} \Phi^{t_j}(D_j) \subset D, \qquad j = 0, 1, \dots$$

and, for all positive $t < t_j$, $\Phi^t(D_j)$ is a sub-domain of one of the Ω_i and is disjoint from D. The discontinuous map on D defined by the ρ_j is the *return map* on D.

The above definition ensures that t_j is the first return time to D, and that the torus map Φ is itself a return map for the domain Ω. In particular, the domain Ω has Φ as its return map, with associated sub-domains Ω_j, unit return times, and translation vectors δ_j given in (31).

Thanks to the identity $\mathcal{R}^q = \mathbf{1}$, we have the following useful result.

Lemma 4.1 *The return map ρ on a domain D may be represented, on each sub-domain D_j, as*

$$\rho_j = \mathcal{T}_{\delta_j} \circ \mathcal{R}^{\hat{t}_j}$$

where $\mathcal{T}$ is the translation operator defined in (26), $\delta_j \in \mathcal{M}^2$ and

$$0 \le \hat{t}_j < q \qquad \hat{t}_j \equiv t_j \,(\mathrm{mod}\ q).$$

The return-map partition $\{D_j\}$ of a domain D may contain a member which is a smaller copy of D, contracted by a factor ω. If this property repeats itself ad infinitum, we have a self-similar family of nested domains, converging toward a limit point in the closure of D. Such behaviour characterizes what we shall call a *scaling domain.*

Def. (*scaling domain*) Let D be a domain, ω an algebraic number of magnitude less than one in $\mathbf{Z}[\lambda]$, and ζ_* a point, which we take to be the origin of coordinates, in the closure of D. D is a *scaling domain, with limit point ζ_* and contraction factor ω*, if there exists an infinite sequence of domains $D^{(n)}$, $n \ge 0$, $D^{(0)} = D$, each equipped with a return map, $\rho^{(n)}$, and a partition $\{D_j^{(n)}\}$, such that for all j,

$$D_j^{(n+1)} = \mathcal{S}_\omega D_j^{(n)}, \tag{32}$$

$$\rho^{(n+1)} \circ \mathcal{S}_\omega D_j^{(n)} = \mathcal{S}_\omega \circ \rho_j^{(n)} D_j^{(n)}, \tag{33}$$

$$\rho_j^{(n+1)} D_j^{(n+1)} = \rho_{j_k}^{(n)} \circ \cdots \circ \rho_{j_0}^{(n)} D_j^{(n+1)} \tag{34}$$

where the subscripts $j_0, \dots, j_k$ depend on j only.

Formula (34) in the above definition implies a linear recursion relation for the return times, as expressed in the following lemma.

Lemma 4.2 *Let D be a scaling domain with associated level-n partitions $\{D_j^{(n)}$, $j = 0, \dots, m\}$. The return times of level $n+1$ are related to those of level n by the linear recursion formula*

$$t_j^{(n+1)} = \sum_{i=0}^{m} \nu_{ji}\, t_i^{(n)} \qquad \nu_{ji} = \sum_{r=0}^{k} \delta_{i,j_r} \tag{35}$$

where δ is Kroneker's delta, and the indices j_r specifies the return path as in (34).

Proof. From (34) we have

$$t_j^{(n+1)} = \sum_{r=0}^{k} t_{j_r}^{(n)}$$

from which the result follows by regrouping the terms. $\square$

For a particular torus map, we would like to be able to prove by induction the existence of scaling — more precisely, the existence of scaling domains — by examining only the first few iterations of the return-map partitioning. The following lemma details the hypotheses that must be verified in order to conclude that we are dealing with a scaling domain.

Lemma 4.3 *A domain D is a scaling domain, with origin ζ_* and contraction factor $\omega \in \mathbf{Z}[\lambda], |\omega| < 1$, if $D^{(0)} \stackrel{\text{def}}{=} D$ and $D^{(1)} \stackrel{\text{def}}{=} S_\omega D$ have respective return maps $\rho^{(0)}$ and $\rho^{(1)}$ and partitions $\{D_j^{(0)}\}$ and $\{D_j^{(1)}\}$ satisfying conditions (32), (33), and (34) for $n = 0$.*

Proof. We proceed by induction. Assuming that the level-N and $N+1$ return map partitions exist and satisfy (32), (33), and (34), we define

$$D_j^{(N+2)} \stackrel{\text{def}}{=} S_\omega D_j^{(N+1)}$$

and

$$\rho_j^{(N+2)} D_j^{(N+2)} = S_\omega \circ \rho_j^{(N+1)} D_j^{(N+1)}.$$

thus establishing equations (32) and (33) for $n = N+1$. Using (32), (33), and (34) for $n = N$, we have

$$\begin{aligned}
\rho_j^{(N+2)} D_j^{(N+2)} &= \rho_j^{(N+2)} \circ S_\omega D_j^{(N+1)} = S_\omega \circ \rho_j^{(N+1)} D_j^{(N+1)} \\
&= S_\omega \circ \rho_{j_k}^{(N)} \circ \cdots \circ \rho_{j_0}^{(N)} D_j^{(N+1)} \\
&= \rho_{j_k}^{(N+1)} \circ \cdots \circ \rho_{j_0}^{(N+1)} \circ S_\omega D_j^{(N+1)} \\
&= \rho_{j_k}^{(N+1)} \circ \cdots \circ \rho_{j_0}^{(N+1)} D_j^{(N+2)},
\end{aligned}$$

which gives us (34) for $n = N+1$.

To complete the proof, we must show that $\rho^{(N+2)}$, defined via the set of $\rho_j^{(N+2)}$, is a well defined return map for $D^{(N+2)} = S_\omega D^{(N+1)}$. From (33) and the scaling of inclusion relations, we have

$$\rho_j^{(N+2)} D_j^{(N+2)} \subset S_\omega D^{(N+1)} = D^{(N+2)},$$

and hence

$$\rho^{(N+2)} D^{(N+2)} \subset D^{(N+2)}.$$

Moreover, from (34) for $n = N+1$, it follows that

$$\rho_j^{(N+2)} D_j^{(N+2)} = \Phi^{t_j^{(N+2)}} D_j^{(N+2)}, \quad j = 0, \ldots, m,$$

where $t_j^{(N+2)} = \sum_{i=0}^{k} t_{j_i}^{(N+1)}$. Because $\rho^{(N+1)}$ is a return map for $D^{(N+1)}$, we know from (34) that $\Phi^t D_j^{(N+2)}$ is disjoint from $D^{(N+1)}$, hence from $D^{(N+2)} =$

$S_\omega D^{(N+1)}$, for all positive $t < t_j^{(N+2)}$ not equal to $\sum_{i=0}^{l} t_{j_i}^{(N+2)}$, some $l < k$. But from the induction hypothesis, for $l < k$, we have

$$\rho_{j_l}^{(N)} \circ \cdots \circ \rho_{j_0}^{(N)} D_j^{(N+1)} \subset D_{j_{l+1}}^{(N)}$$

where

$$D_{j_{l+1}}^{(N)} \cap D^{(N+1)} = \emptyset.$$

Scaling with S_ω, we get that $\rho_{j_l}^{(N+1)} \circ \cdots \circ \rho_{j_0}^{(N+1)} D_j^{(N+2)}$ is disjoint from $D^{(N+2)}$ for $l < k$. Thus $\Phi^t D_j^{(N+2)}$ is disjoint from $D^{(N+2)}$ for all positive $t < t_j^{(N+2)}$, and so the first-return property is verified. $\square$

Once we have identified a scaling domain, it is straightforward to find scaling sequences of periodic orbits associated with it.

Lemma 4.4 *Let D be a scaling domain, with limit point ζ_* and contraction factor ω. Suppose Π is a subdomain of D which is periodic, in the sense that*

$$\Pi = \rho_{j_k} \circ \ldots \circ \rho_{j_0} \Pi$$

for some sequence of integers $(j_0, \ldots, j_k)$, and this is the shortest sequence with this property. Then there exists an infinite sequence of periodic domains $S_\omega^n \Pi$ with return times

$$t_\Pi^{(n+1)} = \sum_i t_{j_i}^{(n)} = \sum_j \nu_j t_j^{(n)} \quad ,$$

where

$$\nu_j = \sum_i \delta_{j j_i}.$$

Proof. We seek to prove by induction that

$$\Pi^{(n)} = \rho_{j_k}^{(n)} \circ \ldots \circ \rho_{j_0}^{(n)} \Pi^{(n)}, \quad n = 0, 1, \ldots, \tag{36}$$

where $\Pi^{(n)} = S_\omega^n \Pi$, and $\rho_j^{(n)}$ and $t_j^{(n)}$ are the return map and return time of the level-n domain $D_j^{(n)}$ associated with the scaling domain D (see the definition). Equation (36) holds for $n = 0$ by hypothesis. Now assume it is valid for $n = N$. Applying S_ω to both sides of (36) with $n = N$ and commuting $S_\omega$through using (33) gives the result for $n = N + 1$. The return time for $\Pi^{(n)}$ is the sum of the return times $t_{j_i}^{(n)}$ for the $\rho_{j_i}^{(n)}$, $i = 0, \ldots, k$ appearing in (36). The formula for $t_\Pi^{(n+1)}$ follows by regrouping terms. $\square$

Note that there is a distinction between the *return time* of a periodic domain Π and the *period* of its points under Φ. For a single-vertex domain, the two are of course identical. Otherwise, it may happen, due to symmetry, that the return time t of a domain is not a multiple of q. In this case, only the centroid has period t, while the period of all other points is the least common multiple of t and q.

5 Proof of scaling for rounding-down models

We now turn to the statement and proof of our main assertions concerning scaling domains and scaling sequences of periodic domains for the 8 models corresponding to rounding-down maps. Theorem 2 (page 4) is an immediate consequence of Proposition 5.2 below, combined with explicit calculation of the algebraic properties of the contraction factors ω appearing in Table V.

5.1 Scaling domains

Proposition 5.1 *For each of the 8 rounding-down maps, each convex set $D^{(0)}$ listed in Table IV is a scaling domain, with the specified limit point ζ_* and contraction factor ω. For each non-negative integer n, and the specified values of j, the convex sets $D_j^{(n)}$ listed in Table IV comprise a return-map partition of $D^{(n)} = \mathcal{S}_\omega^n D^{(0)}$, with the specified return paths, return times, and translation vectors.*

Proof. By Lemma 4.3, it is sufficient to show that

(i) For $n = 0, 1$, $D^{(0)}$ and $D^{(1)} \stackrel{\text{def}}{=} \mathcal{S}_\omega D^{(0)}$ are non-empty domains with partitions

$$D^{(n)} = \bigcup_j D_j^{(n)}\ , \quad D_i^{(i)} \cap D_j^{(n)} = \emptyset \text{ for } i \neq j.$$

(ii) The piecewise affine mapping $\rho^{(0)}$ defined on $D^{(0)}$ by

$$\rho_j^{(0)} D_j^{(0)} \stackrel{\text{def}}{=} \mathcal{T}_{\delta_j^{(0)}} \circ R_{t_j^{(0)}} D_j^{(0)}$$

is a return map.

(iii) The piecewise affine mapping $\rho^{(1)}$ defined on $D^{(1)}$ by

$$\rho_j^{(1)} D_j^{(1)} \stackrel{\text{def}}{=} \rho_{j_k}^{(0)} \circ \cdots \circ \rho_{j_0}^{(0)} D_j^{(1)},$$

with the path indices $j_0, \ldots, j_k$ given (in that order) in Table IV, is a return map.

(iv) For all domains $D_j^{(1)}$ in the partition of $D^{(1)}$, we have

$$\rho_j^{(1)} D_j^{(1)} = \mathcal{T}_{\delta_j^{(1)}} \circ \mathcal{R}_{t_j^{(1)}} D_j^{(1)} = \mathcal{S}_\omega \circ \mathcal{T}_{\delta_j^{(0)}} \circ \mathcal{R}_{t_j^{(0)}} D_j^{(0)}.$$

Note that the defining properties (32) and (34) of a scaling domain follow from the definitions of $D^{(1)}$ and $\rho_j^{(1)}$. Property (33) is a consequence of (iv).

All of the statements (i)-(iv) can be verified explicitly by a finite number of straightforward (if tedious) calculations, which we have performed using the computer algebra system Mathematica. Our procedures comprise the small library of functions defined in Appendix A (see Table III, for a summary), which are sufficiently simple to be understood without familiarity with Mathematica's syntax.

The verification of statements (i)-(iv) was carried out in a set of Mathematica "notebooks" (interactive documents), which can be retrieved at `http://poincare.physics.nyu.edu/ jhl2/ComputerAssistant/`. In Appendix B we present the relevant steps for the main return-map tests in the relatively simple case $p/q = 1/5$.

Proof of (i). The non-triviality of the domain specifications was established by showing (with `vertices`, definition A.4) that each of the listed domains has a non-empty set of vertices. Mutual disjointness of the $D_j^{(n)}$ was verified using `disjoint`.

The property $D^{(n)} = \bigcup_j D_j^{(n)}$ was verified by decomposing $D^{(n)}$ into its constituent subdomains by means of a sequence of binary partitions. If D is a domain and L a line intersecting D, specified by the equation $u^{(m_L)} \cdot \zeta = b_L$, then $D = D_+ \cup D_+$, where $D_\pm$ is the domain obtained from D by adding the constraint $(m_L^\pm b_L)$, i.e., the intersection of D with one of the 2 complementary half-planes bounded by L, one of which contains L itself. Guided by the plots of the relevant domains and subdomains, we have repeated applied this binary splitting process to $D^{(0)}$ and its fragments, each time verifying that one of the resulting subdomains is equal to one of the $D_j^{(0)}$. The process was iterated until all $D_j^{(0)}$ were accounted for, and there were no residual fragments.

Once we had verified the partition of $D^{(0)}$, that of $D^{(1)}$ followed immediately by scale invariance.

Proof of (ii). We must show that

$$\rho_j^{(0)} D_j^{(0)} = \mathcal{T}_{\zeta_*}^{-1} \circ \Phi^{t_j^{(0)}} \circ \mathcal{T}_{\zeta_*} D_j^{(0)}$$

and, moreover, for $t < t_j^{(0)}$,

$$D^{(0)} \cap \mathcal{T}_{\zeta_*}^{-1} \circ \Phi^t \circ \mathcal{T}_{\zeta_*} D_j^{(0)} = \emptyset.$$

Here we have taken into account that $\rho^{(0)}$ and Φ are defined with respect to different coordinate origins. This test was implemented by the function `returntest1` (definition A.15), which yielded a positive result in all cases.

Proof of (iii) and (iv). Using `returntest2` (definition A.16), we have shown that in all cases that $\rho_j^{(1)}$, defined by $\rho_{j_k}^{(0)} \circ \cdots \circ \rho_{j_k}^{(0)}$, maps $D_j^{(1)}$ into $D^{(1)}$ and coincides with $\mathcal{T}_{\delta_j^{(1)}} \circ \mathcal{C}_{t_j^{(1)}}$, $\delta_j^{(1)} = \mathcal{S}_\omega \delta_j^{(0)}$, $t_j^{(1)} \equiv t_j^{(0)} \pmod q$, on $D_j^{(1)}$. In order for the second equality in (iv) to hold, one must have

$$\sum_{i=0}^{k} t_{j_i}^{(0)} \equiv t_j^{(0)} \pmod q,$$

a fact which can easily be verified from Table IV.

The computer verification of the return property does not check for first return. The latter follows, however, from the fact that the images of $D_j^{(1)}$, which start out in $D_{j_0}^{(0)}$, never reenter that domain until the very end, since in each case (see Table IV), the return path is such that $j_i \neq j_0$ for $i > 0$. $\square$

5.2 Periodic domains

Proposition 5.2 *For each of the 8 rounding-down maps, the convex set $\Pi_i^{(0)}, i = 0, \ldots, i_{\max}$ listed in Table V is a periodic domain of nonzero measure, with the specified return time and return path within $D^{(0)}$. The set of domains $\{\Pi_j^{(n)} \stackrel{\text{def}}{=} \mathcal{S}_\omega^n \Pi_j^{(0)},\ n \geq n_0\}$ is a scaling sequence of periodic domains with the specified limit point ζ_* and contraction factor ω. For each map, the orbits of all scaling sequences, together with the finite number of periodic domains listed in Table VI, exhaust the measure of Ω. The periodic domains are mutually disjoint, hence form a partition of $\Omega \setminus \bar{W}$.*

Proof. Due to Lemma 4.4, it is sufficient to verify

(i) $\Pi_i^{(0)}$ is a non-empty subdomain of $D^{(0)}$.

(ii) The domain $\Pi_i^{(0)}$ satisfies

$$\Pi_i^{(0)} = \rho_{j_k}^{(0)} \circ \cdots \circ \rho_{j_0}^{(0)} \Pi_i^{(0)}$$

with the return map for $D^{(0)}$ given in Table IV and the return path $j_0, \ldots, j_k$ listed (in that order) in Table V. The return path is a first-return path.

(iii) The sum over the areas of the orbits of all periodic domains listed in Tables V and VI is equal to the area of Ω, i.e.,

$$\sum_{i=0}^{i_{\max}} \sum_{n=n_0}^{\infty} \mathcal{A}(\Pi_i^{(n)}) t_i^{(n)} + \sum_{\Pi}^{\text{exceptional}} \mathcal{A}(\Pi)\, t(\Pi) = \mathcal{A}(\Omega) = \tau^2.$$

Again we rely on the computer assistant, using the functions of Appendix A, to do the tedious checking of (i)-(iii).

Proof of (i). The nonzero measure of $\Pi^{(0)}$ is obtained by checking for a number of vertices at least 3, using the function `vertices`. The inclusion in $D^{(0)}$ is checked with `subdomain`.

Proof of (ii). The return property is checked using `returntest3` (definition A.17). Since $j_r \neq j_0$ for $r > 0$ (see Table V), the orbit of $\Pi_j^{(0)}$, which starts in $D_{j_0}^{(0)}$, never reenters that domain until the very end. This is sufficient for the first-return property.

Proof of (iii). The return times for $\Pi_j^{(n)}$ are sums of nth powers of integers, and, moreover, from 30, we have

$$\mathcal{A}(\Pi(_j^{(n)})) = \omega^{2n} \mathcal{A}(\Pi_j^{(0)}),$$

so the infinite sum in (iii) is a linear combination of geometric series, which can be evaluated exactly. Here the use of a computer is helpful, but not essential. For each case, we have performed the summations and verified that the total area occupied by the periodic orbits is τ^2.

□

6 Structure of the discontinuity set

In this section we provide two examples of decompositions of the discontinuity set of a torus map, into orbits. We shall also briefly discuss a connection between aperiodic orbits in the discontinuity-set orbits and escape orbits in the dual round-off models.

example	p/q	τ	Ω
I	3/10	$-(1+\sqrt{5})/2$	$(\tau, 0\,]^2$
II	3/8	$-\sqrt{2}/2$	$(\tau, -\tau\,]^2$

In example I, the discontinuity set decomposes, apart from a small number of short-period orbits, into two infinite scaling sequences of periodic open line segments, and two infinite scaling sequences of periodic points, namely the endpoints of the line segments.

Example II is qualitatively different. Once again we obtain scaling sequences of periodic open segments, but now the segment endpoints belong to infinite orbits, and the complement of the closed segments in the base line is a Cantor set. Its one-dimensional Lebesgue measure is zero, and it contains an uncountable infinity of aperiodic orbits. Our recursive analysis provides a symbolic dynamics for the forward and backward evolution of these orbits. Some of the results for this case, including the existence of an infinite orbit of segment endpoints, were obtained previously by Adler *et. al.* [1].

6.1 Example I

Proposition 6.1 *For the torus map defined by*

$$C = \begin{pmatrix} 0 & 1 \\ -1 & -\tau \end{pmatrix}, \qquad \tau = \lambda^{-1} = -\frac{1+\sqrt{5}}{2},$$

acting on $\Omega = (\tau, 0]^2$*, the discontinuity set may be partitioned into a countable set of periodic domains of dimension 1 and 0. The baseline domain* $\mathcal{B} = \{(\zeta_0, \zeta_1) \,|\, \zeta_0 = 0,\, -1 < \zeta_1 \leq 0\}$ *serves as surface of section. Specifically,*

$$\mathcal{B} = \bigcup_{n \geq -1} \left(\Pi_a^{(n)} \cup \Pi_b^{(n)} \cup \Pi_c^{(n)} \cup \Pi_d^{(n)} \right) \cup \Pi_1^{(-1)} \cup \Pi_2^{(-1)} \cup \Pi_3^{(-1)}, \tag{37}$$

where the domains Π_a*–*Π_d *are defined by* $\zeta_0 = 0$ *and*

$$\begin{array}{ll} \Pi_a^{(n)} & \zeta_1 \in (\lambda^{2n+3},\, -\lambda^{2n+4}) \\ \Pi_b^{(n)} & \zeta_1 = -\lambda^{2n+4} \\ \Pi_c^{(n)} & \zeta_1 \in (-\lambda^{2n+4},\, \lambda^{2n+5}) \\ \Pi_d^{(n)} & \zeta_1 = \lambda^{2n+5}, \end{array}$$

and $\Pi_j^{(-1)}$*,* $j = 1, 2, 3$*, are listed in Table VII (b).*

Proof. The map is just that of the rounding-down model with $p/q = 3/10$, so that we have already established the existence and return-map partition of the scaling domain $D^{(0)}$ (data in Table IV), as well as the existence of a full-measure set of periodic orbits based on the pentagonal domains $\Pi_j^{(n)}$ (see data in Table V, and Figure 5). To incorporate the zero-measure orbits of the discontinuity set, we use the refined partition of the fundamental domain Ω listed in Table VII (a) and depicted in Figure 4. The augmented list of periodic domains is given in Table VII (b) and displayed in Figures 6 and 7. The first step of our proof is to verify this partition and the return-map data of the table. We have carried this out using the procedures listed in Appendix A.

That all points of the discontinuity set are images of points of $\mathcal{B}$ under forward or backward iteration of Φ follows from

$$\Omega_5 \subset \Phi^{-1}(\Omega_6 \cup \Omega_7 \cup \Omega_9), \qquad \Omega_7 \subset \Phi^5(\Omega_6), \tag{38}$$

which can be verified directly.

We next show , with computer assistance,

$$\mathcal{B} = \Pi_a^{(-1)} \cup \Pi_b^{(-1)} \cup \Pi_c^{(-1)} \cup \Pi_d^{(-1)} \cup \Pi_1^{(-1)} \cup \Pi_2^{(-1)} \cup \Pi_3^{(-1)} \,\cup\, \Phi^{12} D_3^{(0)} \tag{39}$$

where the scaling subdomain $D_3^{(0)}$ is listed in Table IV. The self-similar structure of $\mathcal{B}$ is inherited from the corresponding structure of $D_3^{(0)}$. With reference to Table VII (b) we have

$$D_3^{(0)} = \Pi_2^{(0)} \cup \Pi_3^{(0)} \cup \Pi_4^{(0)} \cup \Pi_5^{(0)} \cup \rho^{(0)4} D_3^{(1)} \tag{40}$$

and, for all $n \geq 0$ (by scaling)

$$D_3^{(n)} = \Pi_2^{(n)} \cup \Pi_3^{(n)} \cup \Pi_4^{(n)} \cup \Pi_5^{(n)} \cup \rho^{(n)4} D_3^{(n+1)}. \tag{41}$$

The map

$$\rho^{(n)4} = \rho_0^{(n)} \circ \rho_4^{(n)} \circ \rho_0^{(n)} \circ \rho_2^{(n)}$$

has return time divisible by 10, hence preserves the order of the intervals on the parallel line segments $D_3^{(n+1)}$ and $D_3^{(n)}$. From (38), (39), and (40), the images of the $\Pi_j^{(n)}$ on $\mathcal{B}$, given by

$$\left\{\begin{array}{l} \Pi_a^{(n)} \\ \Pi_b^{(n)} \\ \Pi_c^{(n)} \\ \Pi_d^{(n)} \end{array}\right. = \Phi^{12} \circ \rho^{(0)4} \circ \rho^{(1)4} \circ \cdots \circ \rho^{(n-1)4} \left\{\begin{array}{l} \Pi_2^{(n)} \\ \Pi_3^{(n)} \\ \Pi_4^{(n)} \\ \Pi_5^{(n)} \end{array}\right. \qquad n \geq 0$$

partition $\mathcal{B}$ as claimed. The recursive periodic-orbit structure of B is depicted in Figure 8. $\square$

6.2 Example II

We state and prove two results that describe the discontinuity set for the parameters $p/q = 3/8$, $\Omega = (-\tau, \tau]$. The first (Proposition 6.2), describes the decomposition of the discontinuity set into periodic orbits, plus a Cantor set of aperiodic ones. The second (Proposition 6.3), provides a finer characterization of the Cantor orbits.

Proposition 6.2 *The discontinuity set of the torus map*

$$C = \begin{pmatrix} 0 & 1 \\ -1 & -\lambda \end{pmatrix}, \qquad \lambda = \tau^{-1} = -\sqrt{2}, \qquad \Omega = (\tau, -\tau]^2$$

has the baseline $\mathcal{B} = \{-\tau\} \times (\tau, -\tau]$ as surface of section. The periodic domains $\Pi_1^{(-1)}$ and $\Pi_3^{(n)}$, $n \geq 0$, defined in Table IX, are disjoint open segments, whose forward images cover $\mathcal{B}$, apart from a set $\mathcal{C}$ of zero measure. The locations and lengths of all the periodic segments of $\mathcal{B}$ are given, in recursive form, in Table X. The set $\mathcal{C}$, defined recursively in Table X, is a Cantor set of Hausdorff dimension $-\log 5/\log \omega$, containing representatives of uncountably many aperiodic orbits, which include those passing through $(\tau, -\tau)$ and $(-\tau, 0)$.

The aperiodic orbit through $(\tau, -\tau)$ was found in [1].

Proof. The proof will be subdivided into sections.

(a) Generating partition.

We verify that the generating partition of Ω consists of 12 domains, with return time unity (Table VIII (a) and Figure 9). Similarly, we verify that the baseline $\mathcal{B}$ of the discontinuity set decomposes as

$$\mathcal{B} = \Omega_7 \cup \Omega_8 \cup \Omega_9 \cup \Omega_{10},$$

and that the remaining dimension-0 and 1 domains map into $\mathcal{B}$ after at most 2 iterations

$$\Phi(\Omega_4 \cup \Omega_5 \cup \Omega_6) \subset \mathcal{B}, \qquad \Phi^2(\Omega_3) \subset \mathcal{B}, \qquad \Phi^2(\Omega_{11}) \subset \mathcal{B}.$$

(b) Scaling sequences.

The existence and return-map properties of scaling domains and scaling sequences of periodic orbits, with limit point $(-1-\tau,\tau)$ and contraction factor ω^2, where $\omega = \eta^{-2} = 3+4\tau$, are established using steps analogous to those used in the proofs of propositions 5.1 and 5.2. In Tables IX and X we must distinguish between even and odd levels, because the return map of $D^{(n+2)}$ is a rescaled version of $D^{(n)}$, not $D^{(n+1)}$ (even though $D^{(n+1)} = \mathcal{S}_\omega D^{(n)}$, the respective partitions into subdomains differ by more than a rescaling). Because the straightforward definition $D^{(n)} = \mathcal{S}^n_{\omega^2} D^{(0)}$ leads to inconveniently long return path, we treat the cases of even and odd n separately. The price is that we must establish that both $D^{(0)}$ and $D^{(1)} = \mathcal{S}_\omega D^{(0)}$ are scaling domains with limit point $\zeta_* = (-1-\tau,\tau)$ and contraction factor ω^2. By Lemma 4.4, it will be sufficient to show the following:

(i) For $n = 0,1,2$, $D^{(n)} = \mathcal{S}^n_\omega D^{(0)}$ are non-empty domains, with the bounds and return-map partitions listed in Table VIII. In particular,

$$D^{(n)} = \bigcup_j D^{(n)}_j, \qquad D^{(n)}_i \cap D^{(n)}_j = \emptyset, \qquad i \neq j.$$

(ii) The piecewise affine mapping $\rho^{(0)}$ defined by

$$\rho^{(0)}_j D^{(0)}_j \stackrel{\text{def}}{=} \mathcal{T}_{\delta^{(0)}_j} \circ \mathcal{R}^{t^{(0)}_j} D^{(0)}_j,$$

with return times and translation vectors given in Table VIII, satisfies

$$\rho^{(0)}_j D^{(0)}_j = \mathcal{T}^{-1}_{\zeta_*} \Phi^{t^{(0)}_j} \mathcal{T}_{\zeta_*} D^{(0)}_j$$

and is a return map for $D^{(0)}$.

(iii) For $n = 1,2,3$, the map

$$\rho^{(n)}_j D^{(n)}_j \stackrel{\text{def}}{=} \rho^{(n-1)}_{j_k} \circ \cdots \circ \rho^{(n-1)}_{j_0} D^{(n)}_j,$$

with return times and translation vectors given in Table VIII, satisfies

$$\rho^{(n)}_j D^{(n)}_j = \mathcal{T}_{\delta^{(n)}_j} \circ \mathcal{C}^{t^{(n)}_j} D^{(n)}_j,$$

and is a return map for $D^{(n)}$.

(iv) For $n = 2,3$ we have

$$D^{(n)}_j = \mathcal{S}_{\omega^2} D^{(n-2)}_j,$$
$$\delta^{(n)}_j = \omega^2 \delta^{(n-2)}_j, \qquad t^{(n)}_j \equiv t^{(n-2)}_j \pmod 8,$$
$$\rho^{(n)}_j D^{(n)}_j = \mathcal{S}_{\omega^2} \rho^{(n-2)}_j D^{(n-2)}_j.$$

The equations in (i)-(iv) were verified using the computer procedures `returntest1` and `returntest2`. Similarly, the bounds, periodicity and scaling properties of the domains $\Pi^{(n)}_j$ listed in Table IX with $n \leq 3$, were checked using `returntest3`. The extension to arbitrary n follows by Lemma 4.4.

(c) Structure of the baseline.

We begin by reviewing the contents of Table X. The first segment, referring to the fundamental domain Ω, gives the decomposition of the baseline $\mathcal{B}$ into domains Ω_j, $j = 7, 8, 9, 10$ of the generating partition, with each Ω_j being partitioned into domains $\Phi^t D_i^{(-1)}, i = 0, \ldots, 6$. The number of iterations t in each case is given in the 7th column. The various domains are arranged in order of increasing vertical coordinate. Note the possibility of multiple images: e.g., $\Phi^t D_2^{(-1)} \subset \Omega_8$ for $t = 7$ and $t = 11$. The integer $\tilde{t} \equiv t \,(\mathrm{mod}\ 8)$, $0 \leq \tilde{t} < 8$, allows one to infer the orientation of the image relative to the source domain, since the two differ by a generalized rotation $C^{\tilde{t}}$. Thus $\Phi^7 D_2^{(-1)}$ and $\Phi^{11} D_2^{(-1)}$ are oppositely oriented images of $D_2^{(-1)}$ on $\mathcal{B}$. The 5th column of the table gives the coordinates of the pointlike domains, which, due to the linear ordering, also specify the endpoints of the intervening line segments. In the adjoining column, we give the lengths of the image segments.

The substructure of $\mathcal{B}$ is completely specified, recursively, by the remaining segments of Table X ($n = -1$, even n, odd $n \geq 1$). Now, each dimension-zero $D_j^{(n)}$ is decomposed into images under iteration of the return map $\rho^{(n)}$ of various domains $D_i^{(n+1)}$ and, in some cases, a periodic domain $\Pi_j^{(n)}$. The number r of iterations of $\rho^{(n)}$ and the number of Φ-iterations modulo 8, i.e.,

$$\tilde{t} = \left(\sum_{k=1}^{r} t_{j_k}^{(n)} \right) (\mathrm{mod}\ 8) \tag{42}$$

are listed in the last two columns. The coordinates listed in the 5th column now refer to the point-like sub-domains of $D_j^{(n)}$, while the length in the 6th column refers to a segment's forward image along $\mathcal{B}$).

The data contained in columns 1-5 and 7 were verified with computer assistance for all levels up to $n = 1$. For each item, either one is dealing with a periodic domain $\Pi_3^{(n)}$, already treated above, or one starts with a domain $D_j^{(n+1)}$ and iterates the level-n return map $\rho^{(n)}$ as specified in column 7, verifying that the final image domain coincides with that listed in column 5. The length of each segment is obtained by applying the appropriate iterate of the operator $\mathcal{R}$ to obtain a segment parallel to the baseline. The reduced iteration number $\tilde{t}$ is obtained by inserting the return times and return paths of Table VIII into (42). The validity of the table for arbitrary n follows by the usual inductive argument, making use of the commutation relations of the scaling operator (29).

(d) Total length of periodic segments.

We now sum up the lengths of all the periodic segments on $\mathcal{B}$. We note that removing from $\mathcal{B}$ all periodic domains of level less than n leaves a set which is the closure of a certain number $\nu_k^{(n)}$ of open intervals congruent to $\mathcal{D}_k^{(n)}, k = 1, 3, 5, 7$. From Table X, we obtain the recursion relation

$$\begin{pmatrix} \nu_1^{(n+1)} \\ \nu_3^{(n+1)} \\ \nu_5^{(n+1)} \\ \nu_7^{(n+1)} \end{pmatrix} = \begin{pmatrix} 1 & 0 & 2 & 1 \\ 2 & 1 & 2 & 1 \\ 3 & 1 & 2 & 0 \\ 1 & 1 & 1 & 1 \end{pmatrix} \begin{pmatrix} \nu_1^{(n)} \\ \nu_3^{(n)} \\ \nu_5^{(n)} \\ \nu_7^{(n)} \end{pmatrix} \qquad n \geq 2$$

or, more succinctly,

$$\nu^{(n+1)} = R \cdot \nu^{(n)}.$$

Moreover, from the tables, we find explicitly,

$$\nu^{(2)} = (6, 9, 9, 6),$$

an eigenvector of the recursion matrix R with eigenvalue 5. Hence

$$\nu^{(n)} = 5^n \nu^{(2)}, \qquad n = 2, 3, \ldots \tag{43}$$

From Table X, the total length occupied by periodic domains on $\mathcal{B}$ is

$$\sum_{n=1}^{\infty} \nu^{(n)} \Delta^{(n)},$$

where

$$\Delta^{(n)} = \omega^n \qquad\qquad \nu^{(n)} = \begin{cases} \nu_5^{(1)} = 1 & n = 1 \\ \nu_7^{(n)} = 6 \cdot 5^n & n > 1. \end{cases}$$

Thus, the sum over lengths is

$$\omega + 6\omega^2 \sum_{n=0}^{\infty} (5\omega)^n = \omega \left(\frac{1+\omega}{1-5\omega} \right) = \sqrt{2}$$

which is equal to the length of $\mathcal{B}$.

(e) Dimension of the Cantor set.

The Cantor set $\mathcal{C}$ is obtained by systematically removing from $\mathcal{B}$ the periodic intervals of level n, for $n = 1, 2, \ldots$. As noted above, what is left after removal of all periodic intervals of level less than n, is the union of all images of the return-map domains $D_k^{(n)}, k = 1, 3, 5, 7$. From Table X, we see that the lengths of the images in $\mathcal{B}$ of the level-n return-map domains $\mathcal{D}_k^{(n)}$ are

$$\Delta_k^{(n)} = \omega^{n+2} |\tau| \times \begin{cases} 1 & k = 1, 5, 7 \\ 1/\eta & k = 3. \end{cases} \tag{44}$$

If the generalized length

$$\sum \nu_k^{(n)} \left(\Delta_k^{(n)} \right)^d = \frac{3}{25} \omega^{2d} |\tau|^d (7 + 3\eta^{-d})(5\omega^d)^n$$

is to converge to a nontrivial limit for $n \to \infty$, the Hausdorff dimension d must be as stated. $\square$

We turn our attention on the dynamics on the Cantor set $\mathcal{C}$.

Proposition 6.3 *The orbit of every point in $\mathcal{C}$ is dense in $\mathcal{C}$. Furthermore, the orbits of the two points $(-\tau, -\tau)$ and $(-\tau, 0)$ are distinct, and comprise the boundary of $\mathcal{C}^{(n)}$, for all n.*

Proof. Let $p_1, p_2 \in \mathcal{C}$ and $\epsilon > 0$. We wish to find a forward or backward image p_1' of p_1 in $\mathcal{C}$ with the distance between p_1' and p_2 less than ϵ.

We recall that $\mathcal{C}$ is covered by the set $\mathcal{C}^{(n)}$ of images of the domains $D_j^{(n)}$, and that these images are open intervals, of length $\Delta^{(n)} = \omega^2|\tau|$ or $\Delta^{(n)}\omega$, and their endpoints. Hence we choose n such that $\Delta^{(n)} < \epsilon$. Then p_2 is either in an open interval $I \in \mathcal{C}^{(n)}$, or is an endpoint of such an interval. But p_1 has a pre-image p_1'' in some $D_l^{(n+2)}$. That p_1' and p_2 are less than ϵ apart follows from the following property of the return-map domains: for all $n \geq 0, j \in \{1, 3, 5, 7\}, k \in \{1, 2, 3, 4, 5, 7\}, D_j^{(n)}$ contains a forward image of $D_k^{(n+2)}$. For $k = 2, 4$, this is obvious from Table X; for $k = 1, 3, 5, 7$, the number of images of $D_k^{(n+2)}$ in $D_j^{(n)}$

is the kth element of the jth column of the matrix R^2 (see (6.2)), which has only positive entries.

Turning now to the second part of the proposition, we see that the endpoints of level n are all images of $D_2^{(n+1)}$ and $D_4^{(n+1)}$. Moreover, all $D_2^{(m)}, m \geq 2$ lie on the same orbit, which contains $D_7^{(0)} = (-\tau, -\tau)$, and all $D_4^{(m)}, m \geq 2$ lie on the same orbit, which contains $D_9^{(0)} = (-\tau, 0)$.

To prove the distinctness, define the sets

$$\begin{aligned} X &= \{(m_0 + n_0\tau, m_1 + n_1\tau) \,:\, n_0, n_1 \text{ odd}\}, \\ Y &= \{(m_0 + n_0\tau, m_1 + n_1\tau) \,:\, n_0, n_1 \text{ of opposite parity}\}. \end{aligned}$$

It is easy to verify that X and Y are Φ-invariant sets, with $(-\tau, -\tau) \in X$ and $(-\tau, 0) \in Y$. □

We remark that one can construct a round-off type model that supports escape orbits, by exploiting the duality with aperiodic orbits on the discontinuity set.

Consider the round-off model associated with the torus map Φ. One has rounding to the nearest integer, with the midpoint rounded up. Because the points dual to lattice points take the form $m + n\tau$, m, n even integers, no points on the baseline $\mathcal{B}$ or its forward and backward images can be dual to lattice points.

However, if we define Ψ by (18), where the rounding function is rounding down to the nearest *odd* integer, without requiring x, y, or $R(\lambda x) - y$ to be odd. The dual map Φ is unchanged, but the set of dual lattice points is different, and in particular it includes points dual to two infinite orbits through $(-\tau, -\tau)$ and $(-\tau, 0)$. These are necessarily escape orbits, since Φ is invertible.

7 Discussion

We have developed a framework for exact computation with $(\mathbf{L}, \Omega, C)$-maps, in the case in which the eigenvalues of C are roots of unity, while $\mathbf{L}$ and the Ω are defined in terms of algebraic numbers in the corresponding trace (sum of eigenvalues) field. In this setting, it is possible can prove results on a set of orbits of positive measure, with a finite amount of computation. For torus maps which are dual to lattice maps, these results translate into statements on orbits on a lattice, whose density is equal to the aforementioned measure.

When the parameters are algebraic numbers of degree two, we have established —in all maps considered— the existence of orbit scaling, by means of computer-assisted induction. In this case one can prove the periodicity of a set of orbits of full measure. We have shown how the same formalism can be used to characterize the dynamics of the zero-measure discontinuity set, a study which we have performed in two specific cases.

The appearance of units as scaling factors remains unexplained; one of its consequences is that in the coordinates relative to an appropriate limit point, the norm is a scale-invariant function. As a result, a family of self-similar domains can be defined in terms of good rational approximants of the trace λ of the corresponding linear map C. To see this, we write the parameters defining a scaling sequence (e.g., the bounds $b = b^{(n)}$ in (21)) as $b^{(n)} = (x^{(n)} - y^{(n)}\lambda)/a$, with $x^{(n)}$, $y^{(n)}$, a integers, and a independent of n. Considering that $b^{(n)} = \omega^n b^{(0)}$ (equation (28)), and that ω is a unit, we find, taking norms

$$\left(\frac{x^{(n)}}{y^{(n)}} - \lambda\right)\left(\frac{x^{(n)}}{y^{(n)}} - \tilde{\lambda}\right) = \frac{a^2 N(b^{(0)})}{(y^{(n)})^2}.$$

Now, $x^{(n)} - y^{(n)}\lambda$ is bounded, while $x^{(n)}$ and $y^{(n)}$ are unbounded. Thus $x^{(n)}/y^{(n)}$ converges to λ, and so, for some constant c independent of n, we have

$$\left| \frac{x^{(n)}}{y^{(n)}} - \lambda \right| < \frac{c}{|y^{(n)}|^2}$$

as desired.

Beyond the two-dimensional quadratic case, the results for torus maps dual to lattice maps are scarce; there is some evidence that the above phenomena may not generalize to higher dimensions and/or to eigenvalues of higher degree. In [21], a four-dimensional mapping was studied, with roots of unity of degree 6, corresponding to a cubic λ. An exact survey of a set of periodic orbits occupying more than 97% of the measure, revealed no self-similarity. All periodic domains are 'exceptional', and their number appears to grow algebraically with the period.

A Computer assistant

In this appendix, we describe in detail the computational procedures invoked in the computer-assisted proofs of Sections 6 and 7. The various procedures are implemented as Mathematica functions, written so that they can easily be adapted to any high-level computer language capable of arbitrary-precision integer arithmetic and symbolic algebra.

A.1 Mathematica conventions

Function definitions

A function f of arguments $a, b, c, \ldots$ is defined by the expression

```
f[a,b,c,...] := Module[{i,j,...}, statement1; statement2; ...]
```

Here, the statements can depend on the arguments, the local variables `i, j, ...`, and stored constants and variables. When an expression such as `f[x,y,z]` is evaluated, the dummy variables `a, b, c` in the function definition are replaced by `x, y, z`, and the statements separated by semicolons are evaluated in order.

Iterated statements

The iterative expression `For[i = i0, i <= n, i++, statement]` is evaluated as follows: for each successive value of `i` in the sequence `i0, i0 + 1, ..., n`, the `i`-dependent statement is evaluated.

Conditional statements

The expression `If[a, b, c, d]` evaluates to `b` if `a` is true, `c` if `a` is false, and `d` if `a` is indeterminate. In computer-assisted proofs, we always use `If` in such a way that a proof step fails if the condition is indeterminate.

A.2 Algebraic numbers

All numbers encountered in the computer-assisted proofs are of the form $a + b\tau$, where a and b are arbitrary-precision rationals. The quantity τ is treated symbolically. Whenever a polynomial expression in τ is encountered, it is reduced to canonical form by replacing it with the remainder of division by the minimal polynomial L of τ (see equation (12), and Table II).

A.3 Sign of an algebraic number

The sign of an algebraic number $a + b\tau$ is determined using continued fractions [17]. Specifically, from the inequalities

$$\frac{n_{2k}}{d_{2k}} < \tau < \frac{n_{2k+1}}{d_{2k+1}} \qquad k \geq 0 \tag{45}$$

where the rational n_k/d_k is the k-th convergent in the continued fraction expansion of τ, one can bracket $a + b\tau$ between two rapidly converging rational sequences. The convergents are computed recursively from the formulae

$$\frac{n_{2k}}{d_{2k}} = \frac{f_0 n_{2k-1} + n_{2k-2}}{f_0 d_{2k-1} + d_{2k-2}} \qquad \frac{n_{2k+1}}{d_{2k+1}} = \frac{f_1 n_{2k} + n_{2k-1}}{f_1 d_{2k} + d_{2k-1}} \qquad k \geq 1$$

with continued fraction coefficients and initial approximants

p/q	f_0	f_1	n_0	d_0	n_1	d_1
1/5	1	1	1	1	2	1
2/5	1	1	−1	1	−1	2
1/8	2	2	1	1	2	3
3/8	2	2	−1	1	−2	3
1/10	1	1	1	1	1	2
3/10	1	1	−1	1	−2	1
1/12	2	1	1	1	1	2
5/12	2	1	−1	1	−1	2

This suggests the algorithm of the following function definition.

Function Definition A.1

```
signum[a_ + b_ tau] := Module[{m0, m1},
   If[b == 0, Return[Sign[a]]];
   m0 = Sign[num0] * (den0 * a + num0 * b);
   m1 = Sign[num0] * (den1 * a + num1 * b);
   While[Sign[m0] ≠ Sign[m1],
        m0 += f0 * m1;
        m1 += f1 * m0;
        ]; Sign[m0]
   ]
```

The function returns

$$\begin{array}{rl} 0 & \text{if} \quad a = b = 0, \\ 1 & \text{if} \quad a + b\tau > 0, \\ -1 & \text{if} \quad a + b\tau < 0. \end{array}$$

The quantities `f0,f1,num0,den0,num1,den1` are stored constants.

A.4 Domains

The computer assistant uses a data structure `domain[m,s,b]`, where `m, s, b` are B-element lists, to specify the convex sets satisfying the constraints (24). Any function which takes `domain[m,s,b]` as an argument is defined under the assumption that

(i) Each pair of successive constraints $c_k = (m_k, s_k, b_k)$ determines a vertex of the domain (k is a cyclic index).
(ii) Suppose the domain has more than one vertex and that the successive constraint pairs c_{k-1}, c_k and c_k, c_{k+1} both determine the same vertex. Then

$s_k = -s_{k-1} = -s_{k+1} = \mathrm{sign}\lambda$, and hence the vertex is excluded from the domain.
(iii) If the domain has more than one vertex, no more than two pairs of successive constraints determine the same vertex.

These properties imply that the vertices of the domain are cyclically ordered (either clockwise or counter-clockwise), and that, unless the domain is a point, the number of constraints is minimal. As part of our computer-assisted proof, we have verified that each of our tabulated domains satisfies the above rules.

The following function definitions refer to the properties and relations of domains.

Function Definition A.2

```
vertex[m1_, m2_, b1_, b2_] := Module[{},
   FixedPoint[Expand,
   u1inverse[[Mod[m2 - m1 + q, q] + 1]] *
   {uvect[[m2 + 1,2]] * b1 -uvect[[m1 + 1,2]] * b2,
   -uvect[[m2 + 1,1]] * b1 + uvect[[m1 + 1,1]] * b2}
   ]]
```

For two non-parallel constraints, this function uses Cramer's rule to calculate the point $\zeta \in \mathbf{Q}(\tau)^2$ satisfying $u^{(m_j)} \cdot \zeta = b_j, \quad j = 1, 2$. Here `uvect[[i+1,j+1]]` is the jth component of the vector $u^{(i)}$ of the text.

Function Definition A.3

```
vertexconstraint[v_, m0_, s0_, b0_] :=
   signum[s0*(Expand[uvect[[m0 + 1 ]].v] - b0)]
```

This function returns -1, 1, or 0 depending on whether the vertex v lies inside, outside, or on the boundary of the half-plane $s_0 u^{(m_0)} \cdot \zeta < s_0 b_0$.

Function Definition A.4

```
vertices[domain[m_, s_, b_]] :=
   Module[{i, n = Length[m], vx, vlist = {}},
   For[i = 1, i  n, i++,
        vx = vertex[{m[[i]], m[[Mod[i, n] + 1]]},
            {b[[i]], b[[Mod[i, n] + 1]]}];
        If[Not[MemberQ[vlist, vx]], AppendTo[vlist, vx]]
        ];
   vlist
   ]
```

This function returns the set of vertices of the domain d, in cyclic order.

Function Definition A.5

```
subdomain[domain[m_, s_, b_], domain[m1_, s1_, b1_]] :=
   Module[n = Length[m], n1 = Length[m1], v, vc, vtest, etest, i, i1,
        open = lambdasign, closed = -lambdasign,
   For[i = 1, i  n, i++,
        v = vertex[{m[[i]], m[[Mod[i, n] + 1]]},
            {b[[i]], b[[Mod[i, n] + 1]]}];
        For[i1 = 1, i1  n1, i1++,
            vc = vertexconstraint[v, {m1[[i1]], s1[[i1]], b1[[i1]]}];
```

```
            vtest = vc > 0 ||
                (vc == 0 && s1[[i1]] == open &&
                s[[i]] == closed && s[[Mod[i, n] + 1]] == closed);
            If[ Not[vtest === False], Return[False]]
            ];
        If[s[[i]] == open, Continue[]];
        For[i1 = 1, i1  n1, i1++,
            If[s1[[i1]] == closed, Continue[]];
            etest = (m[[i]] == m1[[i1]] && b[[i]] === b1[[i1]]) ||
                ((m[[i]] == m1[[i1]] + q/2 || m[[i]] == m1[[i1]] -q/2)
                && (b[[i]] === -b1[[i1]]));
            If[ Not[etest === False], Return[False]]
            ]
        ];
   True
   ]
```

The function subdomain[d_1,d_2] returns True if d_1 is a subdomain of d_2, and False otherwise. The criteria are
(i) of d_1 must be in the closure of d_2, i.e., the interior of d_1 is contained in d_2.
(ii) vertices of d_1 must be in d_2.
(iii) edges of d_1 must be in d_2.

Function Definition A.6

```
equal[d1_, d2_] :=
   If[subdomain[d1, d2] && subdomain[d2, d1], True, False, False]
```

This function returns True if the two domains are equal, False otherwise.

Function Definition A.7

```
disjoint[d_, domain[m1_, s1_, b1_]] := Module[k,
   For[k = 1, k  Length[m1], k++,
        If[TrueQ[subdomain[d, domain[m1[[k]], -s1[[k]], b1[[k]]]]],
            Return[True]]
        ];
   False
   ]
```

This function returns True if the two domains are disjoint, False otherwise.

Function Definition A.8

```
area[d_] := Module[v, w, k, n, a = 0,
   v = vertices[d];
   n = Length[v]; If[n < 3, Return[0]];
   For[k = 2, k  n, k++, w[k] = v[[k]] - v[[1]]];
   For[k = 2, k < n, k++,
        a += FixedPoint[Expand,
            w[k][[1]] * w[k + 1][[2]] - w[k][[2]] * w[k + 1][[1]]]
        ];
   a * signum[a]/2
   ]
```

This function returns the area, as an algebraic number in $\mathbf{Q}(\tau)$, of a domain with 3 or more vertices.

A.5 Transformations of domains

The following functions implement the elementary transformations of domains described in Section 3.3.

Function Definition A.9

```
rescale[a_, domain[m_, s_, b_]] :=
        domain[m, s, FixedPoint[Expand, a * b]]
```

For $\mathtt{a} \in \mathbf{Z}[\lambda]$, this function rescales all domain bounds by a factor a.

Function Definition A.10

```
rotate[n_, domain[m_, s_, b_]] :=
   domain[Table[Mod[m[[k]] - n, q], {k, Length[m]}], s, b]
```

For integer n, this applies on the domain a generalized rotation C^n.

Function Definition A.11

```
translate[delta_, domain[m_, s_, b_]] :=
   domain[m, s,Table[FixedPoint[Expand,
        b[[k]] + uvect[[m[[k]] + 1]].delta], {k, Length[m]}]]
```

For a given displacement vector delta, this function translates the domain by delta. Here uvect[[m[[k]]+1]] is the vector $u^{(m_{k-1})}$ of the text.

Function Definition A.12

```
map[n_, delta_, dmn_] := translate[delta, rotate[n, dmn]]
```

For a given integer n and displacement vector delta, this function applies the generalized rotation C^n on the domain, then translates it by delta.

Function Definition A.13

```
phimap[d_] := Module[{k, vls},
   For[k = 1, k  Length[dom0], k++,
      If[TrueQ[subdomain[d, dom0[[k]]]],Return[map[1, del0[[k]], d]]]];
   Print["phimap error, ", d]; Abort[] ]
```

Given the stored lists dom0 and del0 of fundamental domains and their respective translation vectors (see Table IV), this function applies the dynamical mapping Φ on the domain d.

A.6 Return tests for scaling domains

We now come to the functions which directly implement steps of the computer assisted proof of Proposition 5.1. First we must store the data of Table V in a set of p/q-dependent constants and functions (see Appendix B for the case $p/q = 1/5$):

limitpoint is the limit point of the scaling domain.

contractionfactor is the contraction factor of the scaling domain.

dom[n_] is the nth domain in the scaling sequence, $D^{(n)}$, $n = 0, 1, \ldots$.

dom[n_,j_] is a member $D_j^{(n)}$ of the return-map partition of $D^{(n)}$.

returntime[n_,j_] is the first-return time $t_j^{(n)}$ for $D_j^{(n)}$.

delta[n_,j_] is the translation vector $\delta_j^{(n)}$ for $D_j^{(n)}$.

returnpath[j_] is the return path for $D_j^{(n)}$.

Function Definition A.14

```
rho[n_,j_,d_]:= map[returntime[n,j],delta[n,j],d]
```

This function applies the return map $\rho_j^{(n)}$ to the domain d.

Function Definition A.15

```
returntest1[n_,j_]:= Module[{d,d1,i},
   d=d1=translate[limitpoint,rho[n,j,dom[n,j]]];
   d2=translate[limitpoint,dom[n]];
   If[subdomain[d1,d2],
      d=phimap[d];
      For[i=2,i<=returntime[n,j],i++,
         If[disjoint[d,d2], d=phimap[d],
           (* else no first return *) Return[False], Return[False]]
          ],
      (* else no return *)Return[False], Return[False]
      ];
   equal[d,d1]
   ]
```

This function tests whether $\rho_j^{(n)}$ is in fact the first-return map for $D_j^{(n)}$, as defined by iterations of the dynamical map Φ.

Function Definition A.16

```
returntest2[n_,j_]:= Module[{d,d1,i,k,path},
   d = dom[n,j];
   path = returnpath[j];
   For[i=1,i<=Length[path],i++,
        k=path[[i]];
        If[subdomain[d,dom[n-1,k]], d=rho[n-1,k,d];
          (* else *) Return[False],Return[False]]
        ];
   d1=rho[n,j,dom[n,j]];
   equal[d,d1]
   ]
```

This function tests whether $\rho_j^{(n)}$ is in fact the first-return map for $D_j^{(n)}$, as defined by iterations of the return map $\rho^{(n-1)}$ along the specified return path.

A.7 Return tests for periodic domains

Prior to testing the return maps of the periodic domains, we store the data of Table VI in a set of p/q-dependent constants and functions in addition to the ones defined above (see Appendix B for the case $p/q = 1/5$).

pi[n_,j_] is the periodic domain $\pi_j^{(n)}$, a subdomain of $D_j^{(n)}$.

orbitpath[j_] is the return path of $\pi_j^{(n)}$.

Function Definition A.17

```
returntest3[n_,j_]:= Module[{d,d1,i,k,path},
   d = d1 = pi[n,j];
   path = orbitpath[j];
   For[i=1,i<=Length[path],i++,
        k=path[[i]];
        If[subdomain[d,dom[n,k]], d = rho[n,k,d];
           (* else *) Return[False],Return[False]]
        ];
   equal[d,d1]
   ]
```

This function tests whether $\pi_j^{(n)}$ is in fact a periodic domain with a specified return path $(j_0,\ldots,j_k)$. Before applying the test, one checks that $j_i \neq j_0, i > 0$, which implies that a return is always a first return.

B Sample of computer-assisted proof

In this appendix we present a detailed, computer assisted verification of some of the principal elements of the proofs of Propositions 5.1 and 5.2, in the case $p/q = 1/5$. Specifically, we show that the scaling domain and periodic domains listed in Tables IV and V have genuine return maps with the claimed partitions, return times and return paths. Below is a list of Mathematica statements, which, when evaluated in the order given (after entering the function definitions of Appendix A), yield positive outcomes for the 3 return-map tests.

B.1 Constants for $p/q = 1/5$

```
p = 1; q = 5;
lambdasign = 1;
num0 = 1; den0 = 1; num1 = 2; den1 = 1;
f0 = 1; f1 = 1;
uvect = {{1, 0}, {0, 1}, {-1, -tau}, {tau, tau}, {-tau, -1}};
u1inverse = {ComplexInfinity, 1, 1 - tau, -1 + tau, -1};
```

B.2 Rule associated with tau

```
tau /:  tau^ n_ := tau^ (n - 2) + tau^ (n - 1) /; n ≥ 2
```

B.3 Generating domain

```
dom[gen] = domain[{0, 1, 0, 1}, {-1, -1, 1, 1}, {0, 0, tau, tau}];
gensubdomains = 4;

dom[gen, 0] = domain[{0, 1, 2}, {-1, -1, -1}, {0, 0, 0}];
dom[gen, 1] = domain[{0, 2, 1, 2}, {-1, 1, -1, -1}, {0, 0, 0, -tau}];
dom[gen, 2] = domain[{0, 1, 2, 0, 2}, {-1, 1, -1, 1, 1}, {0, tau, -2
tau, tau, -tau}];
dom[gen, 3] = domain[{0, 1, 2}, {1, 1, 1}, {tau, tau, -2 tau}];

del[gen, 0] = {0, 0};
del[gen, 1] = {0, tau};
del[gen, 2] = {0, 2 tau};
del[gen, 3] = {0, 3 tau};
```

B.4 Return tests for scaling domain

```
limitpoint = {0, 0};
contractionfactor = 2 - tau;
alpha[n_, a_, b_] := alpha[n, a, b] =
        FixedPoint[Expand, (a + b tau) * contractionfactor^ n];
dom[n_] := [{0, 2, 1, 4}, {-1, 1, -1, -1}, {0, 0, 0, alpha[n, 1, -1]}];


dom[n_, 0] := domain[{0, 3, 1, 4, 1}, {-1, -1, -1, -1, 1},
       {0, alpha[n, 2, -1], 0, alpha[n, 1, -1], -alpha[n, 1, -1]}];
dom[n_, 1] := domain[{0, 2, 1, 4, 3}, {-1, 1, -1, -1, 1},
        {0, 0, 0, alpha[n, 3, -2], alpha[n, 2, -1]}];
dom[n_, 2] := domain[{1, 3, 4}, {-1, 1, 1},
        {0, alpha[n, 2, -1], alpha[n, 3, -2]}];

delta[n_, 0] := {-alpha[n, 1, -1], 0};
delta[n_, 1] := {0, alpha[n, 2, -1]};
delta[n_, 2] := {alpha[n, 2, -1], 0};

returntime[n_, 0] := (1/3)(2 + 10 * 4^ n);
returntime[n_, 1] := 10 * 4^ n;
returntime[n_, 2] := (1/3)(-4 + 70 * 4^ n);

returnpath[0] = {1, 0};
returnpath[1] = {1, 0, 2, 0};
returnpath[2] = {1, 0, 2, 0, 2, 0, 2, 0};

Print[Table[returntest1[0, j], {j, 0, 2}]];
(* Expected output : {True, True, True} *)

Print[Table[returntest2[1, j], {j, 0, 2}]];
(* Expected output : {True, True, True} *)
```

B.5 Return tests for periodic domains

```
pi[n_, 0] := domain[{0, 3, 1, 4, 2}, {1, 1, 1, 1, 1},
        {alpha[n, 5, -3], alpha[n, 4, -2], alpha[n, 2, -1],
         alpha[n, 6, -4], alpha[n, 1, -1]}];
pi[n_, 1] := domain[{0, 3, 1, 4, 2}, {-1, -1, -1, -1, -1},
        {0, alpha[n, 2, -1], 0, alpha[n, 1, -1], alpha[n, 1, -1]}];


orbitpath[0] = {0, 2};
orbitpath[1] = {0};
Print[Table[returntest3[1, j], {j, 0, 1}]];
(* Expected output : {True, True} *)
```

C Tables

TABLE III Fundamental domains, generating partitions, and scaling domains. The coordinates for the scaling domains are relative to the limit points listed in Tables IV (a) and IV (b). #V is the number of vertices of the domain; the translation vector δ_j^{Ω} is defined in (31).

TABLE IV (a) Return-map partitions of the scaling domains for $q \neq 12$. The coordinates are relative to the corresponding limit point ζ^*. The domains $D_j^{(n)}$ and translations $\delta_j^{(n)}$ can be obtained from $D_j^{(0)}$ and $\delta_j^{(0)}$ by multiplying all coordinates by ω^n. The return paths, applicable for $n > 0$, refer to the sequences of domains $D_j^{(n-1)}$. To obtain the return times $t_j^{(n)}$, one may apply the recursion formula (35).

TABLE IV (b) Return-map partitions of the scaling domains for $p/q = 1/12$, and $5/12$ (limit point $\zeta^* = (41 + 72\tau, 41 + 72\tau)$).

TABLE IV (c) Return-map partitions of the scaling domains for $p/q = 5/12$ (limit point $\zeta^* = (\tau, \tau)$).

TABLE V (a) Periodic domains for $p/q \neq 5/12$. The coordinates are relative to the corresponding limit point ζ^*. The domains $\Pi_j^{(n)}$ can be obtained from $\Pi_j^{(0)}$ by multiplying all coordinates by ω^n. The areas scale with a factor ω^2. Each scaling sequence starts with $\Pi_j^{(n_0)}$, with n_0 listed in the fourth column. The return paths refer to sequences of domains $D_j^{(n)}$, and are applicable only for $n > 0$.

TABLE V (b) Periodic domains for $p/q = 5/12$.

TABLE VI (a) Exceptional periodic domains, not belonging to any scaling sequence, for $p/q \neq 5/12$. All coordinates are relative to $(0,0)$. Only domains of positive measure are listed.

TABLE VI (b) Exceptional periodic domains, not belonging to any scaling sequence, for $p/q = 5/12$. All coordinates are relative to $(0,0)$.

TABLE VII (a) Return map data for the generating partition Ω of Example I. The second column lists the number #V of vertices of each subdomain Ω_j; note that not all elements of the generating partition are two-dimensional.

TABLE VII (b) Periodic domain data for Example I. The coordinates for $\Pi_j^{(-1)}$ are relative to $(0,0)$, while those of $\Pi_j^{(n)}$, $n \geq 0$, are relative to the limit point $(0,\tau)$. The symbol α_{rs} denotes $\omega^n(r + s\tau)$.

TABLE VIII (a) Return map data for the domains Ω and $D^{(-1)}$ of Example II. Coordinates for Ω are relative to $(0,0)$, while those of $D_j^{(-1)}$ are relative to the limit point $(-1-\tau,\tau)$.

TABLE VIII (b) Return map data for domains $D^{(n)}$, $n \geq 0$, of Example II. Coordinates are relative to $(-1-\tau,\tau)$. The symbol α_{rs} denotes $\omega^{n+1}(r + s\tau)$.

TABLE VIII (c) Return paths for domains $D^{(n)}$, $n \geq -1$, of Example II. For $n > -1$, the element j_i of the path sequence refers to the subdomain $D_{j_i}^{(n-1)}$; for $n = -1$, it refers to Ω_{j_i}.

TABLE IX Periodic domain data for Example II. Coordinates are relative to $(-1-\tau, \tau)$. The symbol α_{rs} denotes $\omega^{n+1}(r + s\tau)$.

TABLE X (a) Partition of the discontinuity set baseline in Example II. The coordinates in column 5 refer to the point domains and interval endpoints in Ω_j, $j = 7, 8, 9, 10$, and $D_j^{(-1)}$, $j = 0, 1, 2, 4, 5, 6$. For $n = -1$, the coordinates are relative to the limit point $(-1-\tau, \tau)$. The quantities 'length', r_j, and $\tilde{t}_j$ are explained in the text, near equation (42).

TABLE X (b) Continuation of Table X(a). The coordinates in column 5, pertaining to the point domains and interval endpoints in $D_j^{(n)}$, $j = 1, 2, 3, 4, 5, 7$, and n even, are relative to $(-1-\tau, \tau)$. The symbol α_{rs} denotes $\omega^{n+1}(r + s\tau)$.

TABLE X (c) Continuation of Table X(b), for odd n.

Table III

GENERATING PARTITIONS AND SCALING DOMAINS

p/q	domain	$\#V$	bounds	translation $\delta_j^{(\Omega)}$
1/5	Ω	4	$[(0^-,0),(1^-,0),(0^+,\tau),(1^+,\tau)]$	—
	Ω_0	1	$[(0^-,0),(1^-,0),(2^-,0)]$	$(0,0)$
	Ω_1	3	$[(0^-,0),(2^+,0),(1^-,0),(2^-,-\tau)]$	$(0,\tau)$
	Ω_2	5	$[(0^-,0),(1^+,\tau),(2^-,-2\tau),(0^+,\tau),(2^+,-\tau)]$	$(0,2\tau)$
	Ω_3	3	$[(0^+,\tau),(1^+,\tau),(2^+,-2\tau)]$	$(0,3\tau)$
	$D^{(0)}$	3	$[(0^-,0),(2^+,0),(1^-,0),(4^-,1-\tau)]$	—
2/5	Ω	4	$[(0^+,0),(1^+,0),(0^-,\tau),(1^-,\tau)]$	—
	Ω_0	3	$[(0^+,0),(1^-,\tau),(2^+,0)]$	$(0,0)$
	Ω_1	4	$[(0^-,\tau),(1^+,0),(2^-,0),(1^-,\tau)]$	$(0,\tau)$
	$D^{(0)}$	3	$[(1^+,0),(2^-,0),(3^+,1+\tau)]$	—
1/8	Ω	4	$[(0^-,0),(1^-,0),(0^+,\tau),(1^+,\tau)]$	—
	Ω_0	1	$[(0^-,0),(1^-,0),(2^-,0)]$	$(0,0)$
	Ω_1	3	$[(0^-,0),(1^-,0),(2^-,-\tau)]$	$(0,\tau)$
	Ω_2	5	$[(0^-,0),(1^+,\tau),(2^-,-2\tau),(0^+,\tau),(2^+,-\tau)]$	$(0,2\tau)$
	Ω_3	3	$[(0^+,\tau),(1^+,\tau),(2^+,-2\tau)]$	$(0,3\tau)$
	$D^{(0)}$	3	$[(0^+,0),(1^+,0),(2^+,5-7\tau)]$	—
3/8	Ω	4	$[(0^+,0),(1^+,0),(0^-,\tau),(1^-,\tau)]$	—
	Ω_0	3	$[(0^+,0),(1^-,\tau),(2^+,\tau)]$	$(0,-\tau)$
	Ω_1	5	$[(0^-,\tau),(2^+,0),(0^+,0),(2^-,\tau),(1^-,\tau)]$	$(0,0)$
	Ω_2	3	$[(0^-,\tau),(1^+,0),(2^-,0)]$	$(0,\tau)$
	$D^{(0)}$	3	$[(1^-,0),(4^-,0),(7^-,2+3\tau)]$	—
1/10	Ω	4	$[(0^-,0),(1^-,0),(0^+,\tau),(1^+,\tau)]$	—
	Ω_0	1	$[(0^-,0),(1^-,0),(2^-,0)]$	$(0,0)$
	Ω_1	4	$[(0^-,0),(2^+,0),(1^-,0),(2^-,-\tau),(1^+,\tau)]$	$(0,\tau)$
	Ω_2	3	$[(0^+,\tau),(1^+,\tau),(2^+,-\tau)]$	$(0,2\tau)$
	$D^{(0)}$	3	$[(0^+,0),(2^+,5-8\tau),(8^+,0)]$	—
3/10	Ω	4	$[(0^+,0),(1^+,0),(0^-,\tau),(1^-,\tau)]$	—
	Ω_0	3	$[(0^+,0),(1^-,\tau),(2^+,\tau)]$	$(0,-\tau)$
	Ω_1	5	$[(0^-,\tau),(1^-,\tau),(2^-,\tau),(0^+,0),(2^+,0)]$	$(0,0)$
	Ω_2	3	$[(0^-,\tau),(1^+,0),(2^-,0)]$	$(0,\tau)$
	$D^{(0)}$	3	$[(5^-,0),(1^-,0),(7^-,-1)]$	—
1/12	Ω	4	$[(0^-,0),(1^-,0),(0^+,\tau),(1^+,\tau)]$	—
	Ω_0	1	$[(0^-,0),(1^-,0),(2^-,0)]$	$(0,0)$
	Ω_1	3	$[(0^-,0),(2^+,0),(1^-,0),(2^-,-\tau)]$	$(0,\tau)$
	Ω_2	5	$[(0^-,0),(1^+,\tau),(2^-,-2\tau),(0^+,\tau),(2^+,-\tau)]$	$(0,2\tau)$
	Ω_3	3	$[(0^+,\tau),(1^+,\tau),(2^+,-2\tau)]$	$(0,3\tau)$
	$D^{(0)}$	3	$[(0^+,0),(1^+,0),(9^+,-15+26\tau)]$	—
5/12	Ω	4	$[(0^+,0),(1^+,0),(0^-,\tau),(1^-,\tau)]$	—
	Ω_0	3	$[(0^+,0),(1^-,\tau),(2^+,\tau)]$	$(0,-\tau)$
	Ω_1	5	$[(0^-,\tau),(2^+,0),(0^+,0),(2^-,\tau),(1^-,\tau)]$	$(0,0)$
	Ω_2	3	$[(0^-,\tau),(1^+,0),(2^-,0)]$	$(0,\tau)$
	$D_a^{(0)}$	3	$[(4^-,0),(11^-,0),(7^-,209+362\tau)]$	—
	$D_b^{(0)}$	3	$[(6^-,0),(11^-,0),(3^-,209+362\tau)]$	—

Table IV (a)

RETURN-MAP PARTITIONS

p/q	ζ^*	ω	j	$\#V$	domain $D_j^{(0)}$	return path	$t_j^{(0)}$	translation $\delta_j^{(0)}$
1/5	$(0,0)$	$2-\tau$	0	4	$[(0^-,0),(3^-,2-\tau),(1^-,0),(4^-,1-\tau),(1^+,\tau-1)]$	10	4	$(-1+\tau,0)$
			1	3	$[(0^-,0),(2^+,0),(1^-,0),(4^-,3-2\tau),(3^+,2-\tau)]$	1020	10	$(0,2-\tau)$
			2	3	$[(1^-,0),(3^+,2-\tau),(4^+,3-2\tau)]$	$10(20)^3$	22	$(2-\tau,0)$
2/5	$(0,0)$	$1+\tau$	0	3	$[(3^+,1+\tau),(1^-,-1-\tau),(0^+,1+2\tau),(1^+,0),(0^-,\tau)]$	10^2	2	$(\tau,-1-\tau)$
			1	3	$[(0^-,1+2\tau),(1^+,0),(2^-,0)]$	$10^2 1^2$	3	$(-1-\tau,1+2\tau)$
1/8	(τ,τ)	$3-4\tau$	0	4	$[(2^+,5-7\tau),(0^+,0),(3^+,12-17\tau),(1^+,0)]$	$20^4 20$	49	$(0,-5+7\tau)$
			1	2	$[(0^+,0),(3^-,12-17\tau),(1^+,0),(7^-,-12+17\tau)]$	$20^4(20)^2 1020$	128	$(12-17\tau,0)$
			2	3	$[(0^+,0),(1^+,0),(7^+,-12+17\tau)]$	$20^4(20)^4$	118	$(12-17\tau,12-17\tau)$
3/8	$(0,\tau)$	$3+4\tau$	0	4	$[(4^-,0),(2^-,5+7\tau),(1^-,0),(7^-,2+3\tau)]$	$20^4 20$	19	$(2+3\tau,0)$
			1	2	$[(1^-,0),(2^+,5+7\tau),(4^-,0),(6^+,-5-7\tau)]$	$20^4(20)^2 1020$	40	$(0,5+7\tau)$
			2	3	$[(1^-,0),(4^-,0),(6^-,-5-7\tau)]$	$20^4(20)^4$	34	$(-5-7\tau,5+7\tau)$
1/10	(τ,τ)	$1-\tau$	0	4	$[(0^+,0),(4^+,8-13\tau),(8^+,0),(2^+,5-8\tau)]$	10	42	$(-5+8\tau,-5+8\tau)$
			1	3	$[(0^+,0),(2^+,13-21\tau),(8^+,0)]$	1020	70	$(0,-5+8\tau)$
			2	3	$[(2^-,13-21\tau),(8^+,0),(4^-,8-13\tau),(0^+,0))]$	$10(20)^3$	126	$(8-13\tau,8-13\tau)$
3/10	$(0,\tau)$	$2+\tau$	0	4	$[(1^-,0),(3^-,-1-\tau),(5^-,0),(7^-,-1)]$	20	6	$(0,1)$
			1	2	$[(0^-,-2-\tau),(3^+,-1-\tau),(5^-,0),(8^+,1+\tau)]$	2030	19	$(0,2+\tau)$
			2	3	$[(1^-,0),(5^-,0),(7^-,-2-\tau)]$	2040	10	$(1+\tau,0)$
			3	2	$[(0^-,-2-\tau),(2^+,2+\tau),(5^-,0),(7^+,-2-\tau)]$	20403040	27	$(3+2\tau,-1-\tau)$
			4	3	$[(2^-,2+\tau),(5^-,0),(8^-,1+\tau)]$	$20(40)^3$	18	$(0,-1-\tau)$

Table IV (b)

RETURN-MAP PARTITIONS

Abbreviation: $A = 873$, $B = 03$, $C = 378$.

p/q	ζ^*	ω	j	$\#V$	domain $D_j^{(0)}$	return path	$t_j^{(0)}$	translation $\delta_j^{(0)}$
$1/12$	(τ,τ)	$7-12\tau$	0	3	$[(0^+,0),(8^+,-41+71\tau),(9^+,-15+26\tau)]$	ABC	203	$(15-26\tau,0)$
			1	2	$[(0^+,0),(2^-,41-71\tau),(1^+,56-97\tau),$ $(8^-,-41+71\tau)]$	$ABCA18^47CA5C$	888	$(0,-56+97\tau)$
			2	2	$[(0^+,0),(4^-,41-71\tau),(1^+,0),(10^-,-41+71\tau)]$	$ABCA2CA5C$	877	$(0,-41+71\tau)$
			3	4	$[(7^+,-56+97\tau),(10^+,-41+71\tau),$ $(1^+,0),(9^+,-15+26\tau)]$	$ABCA5C$	406	$(41-71\tau,15-26\tau)$
			4	2	$[(2^+,41-71\tau),(1^-,56-97\tau),(10^+,-41+71\tau),$ $(7^-,-56+97\tau)]$	$ABCA5CA18^9$ 6343318^96C	1941	$(71-123\tau,41-71\tau)$
			5	3	$[(2^+,41-71\tau),(10^+,-41+71\tau),(1^+,56-97\tau)]$	$AB(CA5)^2C$	609	$(71-123\tau,41-71\tau)$
			6	2	$[(0^+,0),(5^-,56-97\tau),(1^+,0),(11^-,-56+97\tau)]$	$ABCA78^46CA5C$	888	$(56-97\tau,0)$
			7	4	$[(0^+,0),(5^+,56-97\tau),(1^+,0),(4^+,41-71\tau)]$	$ABCA78^47CA5C$	844	$(-41+71\tau,-56+97\tau)$
			8	3	$[(0^+,0),(1^+,0),(11^+,-56+97\tau)]$	$ABCA78^97CA5C$	1139	$(56-97\tau,0)$
$5/12$	$(41+72\tau,$ $41+72\tau)$	$2+3\tau$	0	3	$[(6^-,0),(3^-,209+362\tau),(10^-,571+989\tau)]$	a	19459	$(209+362\tau,-362-627\tau)$
			1	4	$[(11^-,0),(8^-,571+989\tau),(5^-,780+1351\tau),$ $(3^-,209+362\tau)]$	$a9$	38918	$(571+989\tau,-780-1351\tau)$
			2	2	$[(2^+,-571-989\tau),(11^-,0),$ $(8^+,571+989\tau),(6^-,0)]$	$a79$	57089	$(0,-571-989\tau)$
			3	2	$[(0^-,780+1351\tau),(4^+,-571-989\tau),(6^-,0),$ $(10^+,571+989\tau)]$	$a89$	58245	$(989+1713\tau,-1142-1978\tau)$
			4	2	$[(0^-,780+1351\tau),(5^+,780+1351\tau),$ $(8^-,571+989\tau),(11^+,-780-1351\tau)]$	$a98$	58245	$(989+1713\tau,-1142-1978\tau)$
			5	3	$[(4^-,-571-989\tau),(8^-,571+989\tau),$ $(11^-,-780-1351\tau)]$	$a99$	58377	$(989+1713\tau,-1142-1978\tau)$
			6	4	$[(6^-,0),(2^-,-571-989\tau),(11^-,0),$ $(7^-,-780-1351\tau)]$	$a6169$	76580	$(-571-989\tau,209+362\tau)$
			7	2	$[(2^-,-1351-2340\tau),(1^+,780+1351\tau),$ $(9^-,-780-1351\tau),(7^+,-780-1351\tau)]$	$a612169$	86787	$(-780-1351\tau,0)$
			8	2	$[(6^-,0),(3^+,780+1351\tau),(1^-,780+1351\tau),$ $(9^+,-780-1351\tau)]$	$a613169$	92983	$(780+1351\tau,-1351-2340\tau)$
			9	3	$[(6^-,0),(9^-,-780-1351\tau),(1^-,780+1351\tau)]$	$a615169$	93115	$(780+1351\tau,-1351-2340\tau)$
			a	3	$[(6^-,0),(3^-,780+1351\tau),(11^-,0)]$	$a6101169$	93115	$(780+1351\tau,-1351-2340\tau)$

Table IV (c)

RETURN-MAP PARTITIONS

Abbreviation: $A = 1b^3 1$, $B = A4A01$.

p/q	ζ^*	ω	j	$\#V$	domain $D_j^{(0)}$	return path	$t_j^{(0)}$	translation $\delta_j^{(0)}$
$5/12$	(τ,τ)	$2+3\tau$	0	3	$[(0^-, 571+989\tau), (7^-, 209+362\tau), (4^-, 0)]$	8	6773	$(-209-362\tau, 362+627\tau)$
			1	4	$[(5^-, 780+1351\tau), (7^-, 209+362\tau), (11^-, 0), (2^-, 571+989\tau)]$	87	13546	$(-209-362\tau, 571+989\tau)$
			2	2	$[(11^-, -780-1351\tau), (0^+, 571+989\tau), (4^-, 0), (6^+, -571-989\tau)]$	876	20187	$(0, 571+989\tau)$
			3	2	$[(6^-, -571-989\tau), (5^+, 780+1351\tau), (2^-, 571+989\tau), (11^+, -780-1351\tau)]$	867	20187	$(0, 571+989\tau)$
			4	3	$[(6^-, -571-989\tau), (11^-, -780-1351\tau), (2^-, 571+989\tau)]$	877	20319	$(0, 571+989\tau)$
			5	2	$[(6^-, -571-989\tau), (2^+, 571+989\tau), (11^-, 0), (8^+, -571-989\tau)]$	897	26647	$(-989-1713\tau, 1142+1978\tau)$
			6	2	$[(9^-, 780+1351\tau), (1^+, -780-1351\tau), (4^-, 0), (7^+, 780+1351\tau)]$	$8a7$	26801	$(-780-1351\tau, 1351+2340\tau)$
			7	3	$[(4^-, 0), (9^-, 780+1351\tau), (1^-, -780-1351\tau)]$	$8d7$	26933	$(-780-1351\tau, 1351+2340\tau)$
			8	3	$[(4^-, 0), (11^-, 0), (7^-, 780+1351\tau)]$	$8c7$	26933	$(-780-1351\tau, 1351+2340\tau)$
			9	2	$[(1^-, -780-1351\tau), (3^+, -780-1351\tau), (4^-, 0), (9^+, 780+1351\tau)]$	$8d9c7$	53421	$(-1560-2702\tau, 1351+2340\tau)$
			a	2	$[(3^-, -780-1351\tau), (2^+, 1351+2340\tau), (11^-, 0), (8^+, -1351-2340\tau)]$	$8dac7$	53575	$(-2340-4053\tau, 2702+4680\tau)$
			b	4	$[(4^-, 0), (8^-, -571-989\tau), (9^-, 1560+2702\tau), (1^-, -1560-2702\tau)]$	$8dbc7$	53630	$(-2131-3691\tau, 2131+3691\tau)$
			c	3	$[(3^-, -780-1351\tau), (8^-, -1351-2340\tau), (11^-, 0)]$	$8dcc7$	53707	$(-2340-4053\tau, 2702+4680\tau)$
			d	3	$[(2^-, 1351+2340\tau), (7^-, 1560+2702\tau), (11^-, 0)]$	$8ddc7$	53707	$(-2340-4053\tau, 2702+4680\tau)$
			e	2	$[(2^-, 1351+2340\tau), (1^+, -1560-2702\tau), (11^-, 0), (7^+, 1560+2702\tau)]$	$8dec7$	53993	$(-1560-2702\tau, 2702+4680\tau)$
			f	2	$[(1^-, -1560-2702\tau), (3^+, -1560-2702\tau), (4^-, 2131+3691\tau), (9^+, 1560+2702\tau)]$	$8dbebc7$	80613	$(-3120-5404\tau, 2702+4680\tau)$
			g	4	$[(0^-, -3691-6393\tau), (3^-, -1560-2702\tau), (8^-, -571-989\tau), (11^-, 0)]$	$8dbbBAbbc7$	244544	$(-989-1713\tau, -989-1713\tau)$
			h	4	$[(6^-, 3691+6393\tau), (10^-, -7173-12424\tau), (11^-, 0), (3^-, -1560-2702\tau)]$	$8dbbBBAbbc7$	348666	$(-5251-9095\tau, 1922+3329\tau)$
			i	2	$[(11^-, 0), (0^+, -3691-6393\tau), (3^-, -1560-2702\tau), (6^+, 3691+6393\tau)]$	$8dbbBA5BAbbc7$	402015	$(0, -3691-6393\tau)$
			j	2	$[(4^-, 7173+12424\tau), (2^+, 3482+6031\tau), (11^-, 0), (8^+, -3482-6031\tau)]$	$8dbbBBA2BBAbbc7$	608839	$(-6031-10446\tau, 6964+12062\tau)$
			k	3	$[(4^-, 7173+12424\tau), (8^-, -3482-6031\tau), (11^-, 0)]$	$8dbbBBA01BBAbbc7$	608971	$(-6031-10446\tau, 6964+12062\tau)$
			l	3	$[(2^-, 3482+6031\tau), (6^-, 3691+6393\tau), (11^-, 0)]$	$8dbbBBA4BBAbbc7$	608971	$(-6031-10446\tau, 6964+12062\tau)$
			m	2	$[(6^-, 3691+6393\tau), (4^+, 7173+12424\tau), (3^-, -12424-21519\tau), (10^+, -7173-12424\tau)]$	$8dbbBBA5BBAbbc7$	610259	$(-12424-21519\tau, 7173+12424\tau)$

TABLE V (a)

PERIODIC DOMAINS

p/q	ζ^*	ω	n_0	j	ret. path	$t_j^{(n)}$	domain $\Pi_j^{(0)}$	area
$1/5$	$(0,0)$	$2-\tau$	-1	0	02	$2(40\cdot 4^n-1)/3$	$[(0^+,5-3\tau),(3^+,4-2\tau),(1^+,2-\tau),(4^+,6-4\tau),(2^+,1-\tau)]$	$(322\tau-521)/2$
			0	1	0	$(20\cdot 4^n+4)/6$	$[(0^-,0),(3^-,2-\tau),(1^-,0),(4^-,1-\tau),(2^-,1-\tau)]$	$(18\tau-29)/2$
$2/5$	$(0,0)$	$1+\tau$	0	0	0	$(20\cdot 4^n+4)/12$	$[(0^+,1+2\tau)),(1^+,0),(2^+,1+\tau),(3^+,1+\tau),(4^+,0)]$	$(18+29\tau)/2$
				1	1	$(20\cdot 4^n-2)/6$	$[(0^-,1+2\tau)),(1^-,1+2\tau),(2^-,0),(3^-,2+3\tau),(4^-,0)]$	$(47+76\tau)/2$
$1/8$	(τ,τ)	$3-4\tau$	-1	0	0	$6\cdot 9^{n+1}-5$	$[(0^+,0),(3^+,12-17\tau),(6^+,12-17\tau),(1^+,0),(4^+,17-24\tau),(7^+,5-7\tau),(2^+,5-7\tau),(5^+,17-24\tau)]$	$(3940-5571\tau)/2$
				1	20	$18\cdot 9^{n+1}+5$	$[(0^+,0),(3^+,-29+41\tau),(6^+,-29+41\tau),(1^+,0),(4^+,-41+58\tau),(7^+,-12+17\tau),(2^+,-12+17\tau),(5^+,-41+58\tau)]$	$(22964-32476\tau)/2$
$3/8$	$(0,\tau)$	$3+4\tau$	-1	0	0	$18\cdot 9^n+1$	$[(0^-,7+10\tau),(1^-,0),(2^-,5+7\tau),(3^-,5+7\tau),(4^-,0),(5^-,7+10\tau),(6^-,2+3\tau),(7^-,2+3\tau)]$	$338+478\tau$
				1	20	$54\cdot 9^n-1$	$[(0^-,-17-24\tau),(1^-,0),(2^-,-12-17\tau),(3^-,-12-17\tau),(4^-,0),(5^-,-17-24\tau),(6^-,-5-7\tau),(7^-,-5-7\tau)]$	$1970+2786\tau$
$1/10$	(τ,τ)	$1-\tau$	-1	0	02	$28(20\cdot 4^n-2)/3$	$[(5^+,-21+34\tau),(1^+,-5+8\tau),(7^+,-26+42\tau),(3^+,-8+13\tau),(9^+,-16+26\tau)]$	$(15127-24476\tau)/2$
			0	1	0	$7(20\cdot 4^n+16)/6$	$[(0^+,0),(6^+,5-8\tau),(2^+,5-8\tau),(8^+,0),(4^+,8-13\tau)]$	$(843-1364\tau)/2$
$3/10$	$(0,\tau)$	$2+\tau$	-1	0	04	$(80\cdot 4^n-8)/3$	$[(0^-,1+\tau),(2^-,4+2\tau),(4^-,1\tau),(6^-,3+2\tau),(8^-,2+2\tau)]$	$(-199-123\tau)/2$
			0	1	0	$(10\cdot 4^n+8)/3$	$[(1^-,0),(3^-,-1-\tau),(5^-,0),(7^-,-1),(9^-,-1)]$	$(-11-7\tau)/2$
$1/12$	(τ,τ)	$7-12\tau$	0	0	7	$2(612\cdot 25^{n+1}-45\cdot 4^{n+1}-350)/35$	$[(0^+,0),(5^+,56-97\tau),(8^+,56-97\tau),(1^+,0),(4^+,41-71\tau),(9^+,41-71\tau)]$	$(29681-51409\tau)/2$
				1	033533	$12(306\cdot 25^{n+1}-180\cdot 4^{n+1}+175)/35$	$[(0^+,0),(5^+,-97+168\tau),(8^+,-41+71\tau),(9^+,-15+26\tau)]$	$(70226-121635\tau)/6$
				2	88737	$4(306\cdot 25^{n+1}+9\cdot 4^{n+1}-35)/7$	$[(0^+,0),(7^+,153-265\tau),(4^+,306-530\tau),(11^+,-56+97\tau),(8^+,56-97\tau),(3^+,265-459\tau)]$	$(413403-716035\tau)/2$
				3	8	$(306\cdot 25^{n+1}+72\cdot 4^{n+1}+35)/7$	$[(1^+,0),(8^+,-362+627\tau),(3^+,-153+265\tau),(10^+,-362+627\tau),(5^+,-418+724\tau),(0^+,-56+97\tau),(7^+,-265+459\tau),(2^+,-56+97\tau),(9^+,-265+459\tau)\ (4^+,-265+459\tau),(11^+,-56+97\tau),(6^+,-418+724\tau)]$	$(3912488-6776628\tau)/2$

Table V (b)

PERIODIC DOMAINS

Abbreviations: $J = jjj242$, $K = jjj2022$

p/q	ζ^*	ω	n_0	j	return path	$t_j^{(n)}$	domain $\Pi_j^{(0)}$	area
$5/12$	(τ,τ)	$2+3\tau$	-1	0	$022J(JK)^3 (KJ)^2 jjj2$	$2499840\cdot 4^n - 228$	$[4^-, -10864-18817\tau), (11^-, -6602-11435\tau), (8^-, 21157+36645\tau), (7^-, 5251+9095\tau)]$	$(2642885282+4577611587\tau)/6$
			-1	1	022422	$80640\cdot 4^n + 636$	$[0^-, 571+989\tau), (7^-, 209+362\tau), (4^-, 0), (3^-, 1351+2340\tau)]$	$(13623482+23596563\tau)/6$
			-2	2	$2jjj$	$174720\cdot 4^n - 284$	$[(7^-, -571-989\tau), (6^-, -1351-2340\tau), (3^-, -4471-7744\tau), (2^-, 571+989\tau), (11^-, 0), (10^-, -4262-7382\tau)]$	$(80198051+138907099\tau)/2$
			-3	3	$allalalaalal$	$645120\cdot 4^n - 636$	$[(0^-, -780-1351\tau), (1^-, 4262+7382\tau), (4^-, 5042+8733\tau), (9^-, 3691+6393\tau)]$	$(189750626+328657725\tau)/6$
			-1	4	$allalajcjl$	$1093680\cdot 4^n - 1500$	$[(0^-, -780-1351\tau), (4^-, 5042+8733\tau), (7^-, -4262-7382\tau)]$	$(-408855776-708158977\tau)/12$
			-1	5	$alajffjlala$	$1093680\cdot 4^n - 1500$	$[(1^-, 1351+2340\tau), (5^-, -2131-3691\tau), (10^-, -7953-13775\tau)]$	$(-408855776-708158977\tau)/12$
			-1	6	$ajejl$	$564480\cdot 4^n - 1140$	$[(0^-, -780-1351\tau), (3^-, -780-1351\tau), (7^-, -4262-7382\tau), (8^-, -4262-7382\tau)]$	$(299303201+518408351\tau)/6$
			-1	7	hjj	$352800\cdot 4^n - 996$	$[(0^-, -3691-6393\tau), (3^-, -1560-2702\tau), (8^-, -571-989\tau), (11^-, 0)]$	$(101687054+176127144\tau)/6$
$5/12$	$(41+72\tau, 41+72\tau)$	$2+3\tau$	0	0	$088a88$	$(12/7)(132450\cdot 5^n + 4736\cdot(-2)^n - 973)$	$[(3^-, 209+362\tau), (10^-, 571+989\tau), (7^-, 1351+2340\tau), (6^-, 0)]$	$(13623482+23596563\tau)/6$
			-1	1	3	$(1/7)(529800\cdot 5^n + 2368\cdot(-2)^n + 3892)$	$[(6^-, 0), (7^-, -780-1351\tau), (10^-, -780-1351\tau), (11^-, 0), (2^-, -571-989\tau), (3^-, -571-989\tau)]$	$(5757961+9973081\tau)/2$

Table VI (a)

EXCEPTIONAL PERIODIC DOMAINS

p/q	j	$\#V$	t_j	domain Π_j	area
$1/5$	0	5	1	$[(0^-,0),(2^-,-\tau),(4^-,-\tau),(1^-,0),(3^-,1)]$	$(3\tau-4)/2$
	1	5	1	$[(1^+,\tau),(4^+,-\tau),(2^+,-\tau),(0^+,\tau),(3^+,2+\tau)]$	$(2\tau-1)/2$
	2	5	1	$[(0^+,\tau),(2^+,-2\tau),(4^+,-2\tau),(1^+,\tau),(3^+,3+\tau)]$	$(7\tau-11)/2$
$2/5$	0	5	1	$[(0^-,\tau),(1^-,\tau),(2^-,0),(3^-,1+\tau),(4^-,0)]$	$(7+11\tau)/2$
$1/8$	0	8	1	$[(0^-,0),(3^-,1-\tau),(6^-,1-\tau),(1^-,0),$ $(4^-,1-2\tau),(7^-,-\tau),(2^-,-\tau),(5^-,1-2\tau)]$	$10-14\tau$
	1	8	1	$[(0^+,\tau),(3^+,2-\tau),(6^+,2-\tau),(1^+,\tau),$ $(4^+,2-3\tau),(7^+,-\tau),(2^+,-\tau),(5^+,2-3\tau)]$	$20-28\tau$
	2	4	4	$[(0^-,0),(5^-,2-3\tau),(3^+,1-\tau),(4^-,2-3\tau),(1^-,0),(2^+,0)]$	$(17-24\tau)/2$
$1/10$	0	10	1	$[(0^-,0),(3^-,1-2\tau),(6^-,2-4\tau),(9^-,-\tau),(2^-,-\tau),$ $(5^-,2-4\tau),(8^-,1-2\tau),(1^-,0),(4^-,2-3\tau),(7^-,2-3\tau)]$	$65\tau-40$
	1	10	1	$[(0^+,\tau),(3^+,2-3\tau),(6^+,4-7\tau),(9^+,-\tau),(2^+,-\tau),$ $(5^+,4-7\tau),(8^+,2-3\tau),(1^+,\tau),(4^+,4-5\tau),(7^+,4-5\tau)]$	$170\tau-105$
	2	5	2	$[(1^+,\tau),(5^+,3-5\tau),(9^+,-\tau),(3^+,1-2\tau),(7^+,3-4\tau)]$	$(123-199\tau)/2$
	3	4	5	$[(5^+,0),(9^+,-3+4\tau),(0^+,-3+5\tau),(4^+,\tau)]$	$34-55\tau$
$1/12$	0	12	1	$[(0^-,0),(5^-,2-3\tau),(10^-,1-\tau),(3^-,1-\tau),(8^-,2-3\tau),(1^-,0),$ $(6^-,2-4\tau),(11^-,-\tau),(4^-,1-3\tau),(9^-,1-3\tau),(2^-,-\tau),(7^-,2-4\tau)]$	$52-90\tau$
	1	12	1	$[(0^+,\tau),(5^+,4-5\tau),(10^+,2-\tau),(3^+,2-\tau),(8^+,4-5\tau),(1^+,\tau),$ $(6^+,4-7\tau),(11^+,-\tau),(4^+,2-5\tau),(9^+,2-5\tau),(2^+,-\tau),(7^+,4-7\tau)]$	$156-270\tau$
	2	12	1	$[(0^+,\tau),(5^+,6-8\tau),(10^+,3-2\tau),(3^+,3-2\tau),(8^+,6-8\tau),(1^+,\tau),$ $(6^+,6-11\tau),(11^+,-2\tau),(4^+,3-8\tau),(9^+,3-8\tau),(2^+,-2\tau),(7^+,6-11\tau)]$	$388-672\tau$
	3	4	96	$[(3^-,5-8\tau),(6^+,5-9\tau),(5^+,5-8\tau),(8^-,6-10\tau)]$	$(362-627\tau)/6$
	4	8	6	$[(0^-,0),(4^+,2-4\tau),(9^+,2-4\tau),(1^-,0),$ $(6^-,5-9\tau),(10^+,1-\tau),(3^+,1-\tau),(7^-,5-9\tau)]$	$(276-478\tau)/3$
	5	6	6	$[(0^-,0),(2^+,0),(1^-,0),(6^-,4-7\tau),(5^+,3-5\tau),(7^-,4-7\tau)]$	$(97-168\tau)/3$
	6	6	4	$[(0^-,0),(5^-,3-5\tau),(8^-,3-5\tau),(1^-,0),(4^-,2-4\tau),(9^-,2-4\tau)]$	$41-71\tau$
	7	6	4	$[(2^+,-\tau),(7^+,5-9\tau),(10^+,2-2\tau),(3^+,2-2\tau),(6^+,5-9\tau),(11^+,-\tau)]$	$(153-265\tau)/2$

Table VI (b)

EXCEPTIONAL PERIODIC DOMAINS

p/q	j	$\#V$	t_j	domain Π_j	area
5/12	0	4	30	$[(0^-, 2+4\tau), (1^-, 2+4\tau), (6^-, 2+3\tau), (7^-, 2+3\tau)]$	$(97+168\tau)/3$
	1	12	13001	$[(0^-, 155+269\tau), (1^-, 1480+2564\tau), (2^-, 192+333\tau),$ $(3^-, 1098+1902\tau), (4^-, 817+1415\tau), (5^-, 398+689\tau),$ $(6^-, 1405+2433\tau), (7^-, 80+138\tau), (8^-, 1368+2369\tau),$ $(9^-, 462+800\tau), (10^-, 743+1287\tau), (11^-, 1162+2013\tau)]$	$27246964+47193126\tau$
	2	12	355	$[(0^-, 2+4\tau), (1^-, -80-138\tau), (2^-, -17-29\tau),$ $(3^-, -44-76\tau), (4^-, -60-104\tau), (5^-, -5-9\tau),$ $(6^-, -84-146\tau), (7^-, -2-4\tau)(8^-, -65-113\tau),$ $(9^-, -38-66\tau), (10^-, -22-38\tau), (11^-, -77-133\tau)]$	$75268+130368\tau$
	3	12	473	$[(0^-, 2+4\tau), (1^-, 114+198\tau), (2^-, 9+16\tau),$ $(3^-, 79+137\tau), (4^-, 63+109\tau), (5^-, 21+36\tau),$ $(6^-, 110+190\tau), (7^-, -2-4\tau), (8^-, 103+178\tau),$ $(9^-, 33+57\tau), (10^-, 49+85\tau), (11^-, 91+158\tau)]$	$140452+243270\tau$
	4	12	7	$[(0^-, -4-6\tau), (1^-, -4-6\tau), (2^-, -1-\tau),$ $(3^-, -6-10\tau), (4^-, 0), (5^-, -5-9\tau),$ $(6^-, -2-4), (7^-, -2-4\tau), (8^-, -5-9\tau),$ $(9^-, 0), (10^-, -6-10\tau), (11^-, -1-\tau)]$	$388+672\tau$
	5	8	9	$[(1^-, \tau), (2^-, -3-4\tau), (4^-, -1-\tau), (5^-, -3-5\tau),$ $(7^-, -3-6\tau), (8^-, -\tau), (10^-, -2-4\tau), (11^-, 0)]$	$(82+142\tau)/3$

Table VII (a)

EXAMPLE I: GENERATING PARTITION

$\Omega = [(0^-,\tau),(1^-,\tau),(0^+,0),(1^+,0)]$

j	$\#V$	domain Ω_j	$t_j^{(n)}$	$\tilde{t}_j^{(n)}$	$\delta_j^{(n)}$
0	3	$[(1^-,\tau),(5^-,0),(7^-,-\tau)]$	1	1	$(0,-\tau)$
1	5	$[(0^-,\tau),(1^-,\tau).(2^-,\tau),(5^-,0),(7^-,0)]$	1	1	$(0,0)$
2	3	$[(0^-,\tau),(2^-,0),(6^-,0)]$	1	1	$(0,\tau)$
3	2	$[(0^-,\tau),(2^+,0),(5^-,0),(7^+,0)]$	1	1	$(0,0)$
4	2	$[0^-,-1),(2^+,\tau),(5^-,0),(7^+,-\tau)]$	1	1	$(0,-\tau)$
5	2	$[(0^-,\tau),(1^+,0),(5^-,0),(6^+,0)]$	1	1	$(0,\tau)$
6	2	$[(1^-,-1),(0^+,0),(6^-,0),(5^+,0)]$	1	1	$(0,0)$
7	2	$[(1^-,\tau),(0^+,0),(6^-,1),(5^+,0)]$	1	1	$(0,-\tau)$
8	1	$[(0^+,0),(2^+,0),(5^+,0),(7^+,0)]$	1	1	$(0,0)$
9	1	$[(0^+,0),(2^+,\tau),(5^+,0),(7^+,-\tau)]$	1	1	$(0,-\tau)$

Table VII (b)

EXAMPLE I: PERIODIC DOMAINS

n	j	domain $\Pi_j^{(n)}$	return time	return path
-1	0	$[(0^-,\tau),(2^-,1+\tau),(4^-,1),(6^-,1),(8^-,1+\tau)]$	4	
	1	$[(0^+,0),(1^+,0),(5^+,0),(6^+,0)]$	1	
	2	$[(0^+,0),(1^-,-1),(5^+,0),(6^-,-1-\tau)]$	5	
	3	$[(0^+,0),(1^+,1+\tau),(5^+,0),(6^+,-1-\tau)]$	7	
	a	$[(0^+,0),(1^-,1+\tau),(5^+,0),(6^-,-2-\tau)]$	25	
	b	$[(0^+,0),(1^+,2+\tau),(5^+,0),(6^+,-2-\tau)]$	13	
	c	$[(0^+,0),(1^-,2+\tau),(5^+,0),(6^-,-3-2\tau)]$	25	
	d	$[(0^+,0),(1^+,3+2\tau),(5^+,0),(6^+,-3-2\tau)]$	17	
$n \geq 0$	0	$[(0^-,\alpha_{11}),(2^-,\alpha_{42}),(4^-,\alpha_{10}),(6^-,\alpha_{32}),(8^-,\alpha_{22})]$	$4^{n+2}\cdot 5/3-8/3$	04
	1	$[(1^-,0),(3^-,-\alpha_{11}),(5^-,0),(7^-,-\alpha_{10}),(9^-,-\alpha_{10})]$	$4^{n}\cdot 10/3+8/3$	0
	2	$[(2^+,\alpha_{21}),(1^-,\alpha_{53}),(7^+,-\alpha_{21}),(6^-,\alpha_{32})]$	$4^{n+2}\cdot 10/3+35/3$	3020
	3	$[(2^+,\alpha_{21}),(1^+,\alpha_{53}),(7^+,-\alpha_{21}),(6^+,-\alpha_{53})]$	$4^{n+2}\cdot 5/3+19/3$	30
	4	$[(2^+,\alpha_{21}),(1^-,-\alpha_{85}),(7^+,-\alpha_{21}),(6^-,-\alpha_{53})]$	$4^{n+2}\cdot 20/3-5/3$	30404040
	5	$[(2^+,\alpha_{21}),(1^+,-\alpha_{85}),(7^+,-\alpha_{21}),(6^+,\alpha_{85})]$	$4^{n+2}\cdot 10/3+11/3$	3040

Table VIII (a)

EXAMPLE II: PRE-SCALING RETURN-MAP PARTITIONS

$\Omega = [(0^-,\tau),(0^+,-\tau),(1^-,\tau),(1^+,-\tau)]$

$D^{(-1)} = [(1^-,0),(4^-,-1),(6^-,0)]$

n	j	domain $D_j^{(n)}$	t_j	$\tilde{t}_j$	δ_j
	0	$[(1^-,\tau),(4^-,\tau),(6^-,-\tau)]$	1	1	$(0,-2\tau)$
	1	$[(0^-,\tau),(1^-,\tau),(2^-,\tau),(4^-,\tau),(5^-,\tau),(6^-,\tau)]$	1	1	$(0,-2\tau)$
	2	$[(0^-,\tau),(5^-,\tau),(2^-,-\tau)]$	1	1	$(0,0)$
	3	$[(2+,-\tau),(0^-,\tau),(6+,\tau),(5^-,\tau)]$	1	1	$(0,2\tau)$
	4	$[(1+,-\tau),(0^-,-\tau),(5+,\tau),(4^-,-1-\tau)]$	1	1	$(0,0)$
Ω	5	$[(1+,-\tau),(2+,-\tau),(5+,\tau),(6+,\tau)]$	1	1	$(0,2\tau)$
	6	$[(1+,-\tau),(0^-,1+\tau),(5+,\tau),(4^-,\tau)]$	1	1	$(0,0)$
	7	$[(0+,-\tau),(1+,-\tau),(4+,\tau),(5+,\tau)]$	1	1	$(0,0)$
	8	$[(0+,-\tau),(1^-,0),(4+,\tau),(5^-,\tau)]$	1	1	$(0,0)$
	9	$[(0+,-\tau),(1+,0),(4+,\tau),(5+,0)]$	1	1	$(0,0)$
	10	$[(0+,-\tau),(1^-,\tau),(4+,\tau),(5^-,0)]$	1	1	$(0,-2\tau)$
	11	$[(2+,\tau),(1^-,\tau),(6+,-\tau),(5^-,0)]$	1	1	$(0,-2\tau)$
	0	$[(0^-,3+3\tau),(3^+,-1),(4^-,-1),(7^+,1)]$	13	5	$(-3-6\tau,4+6\tau)$
	1	$[(0^+,3+3\tau),(1^+,-4-6\tau),(4^+,-3-3\tau),(5^+,4+6\tau)]$	22	6	$(7+10\tau,-5-6\tau)$
	2	$[(1^-,0),(3^+,-1),(5^-,4+6\tau),(7^+,1)]$	12	4	$(4+4\tau,-4-6\tau)$
	3	$[(0^-,-1-2\tau),(1^-,0),(3^-,-1),(4^-,-1),(6^-,0)]$	2	2	$(1,1)$
-1	4	$[(0^+,-1-2\tau),(2^+,-3-4\tau),(4^+,1+2\tau),(6^+,3+4\tau)]$	13	5	$(1,0)$
	5	$[(0^+,-1-2\tau),(1^-,0),(4^+,1+2\tau),(7^-,-1-2\tau)]$	6	6	$(-1-2\tau,1+2\tau)$
	6	$[(0^+,-1-2\tau),(2^-,-3-4\tau),(4^+,1+2\tau),(6^-,0)]$	13	5	$(5+6\tau,-4-6\tau)$
	7	$[(6^-,0),(4^-,1+2\tau),(1^-,0)]$	3	3	$(2+2\tau,-1-2\tau)$
	8	$[(4^-,-1),(1^-,0),(7^-,1)]$	3	3	$(2,1)$

Table VIII (b)

EXAMPLE II: RETURN-MAP PARTITIONS

$D^{(n)} = [(1^-,0),(4^-,-\alpha_{1,-2})(6^-,0)]$

n	j	domain $D_j^{(n)}$	t_j	$\tilde{t}_j$	δ_j
$n \geq 0$ even	0	$[(4^-,-\alpha_{1,-2}),(1^-,0),(7^-,1),(6^-,0)]$	$3\cdot 9^n$	3	$(\alpha_{2,-2},\alpha_{1,-2})$
	1	$[(3^+,-1),(1^-,\alpha_{22}),(7^+,1),(6^-,0)]$	$36\cdot 9^n - 4\cdot 5^n$	0	$(\alpha_{22},-\alpha_{22})$
	2	$[(1^+,\alpha_{34}),(2^+,-\alpha_{22}),(5^+,-\alpha_{34}),(6^+,\alpha_{22})]$	$(177\cdot 9^n - 22\cdot 5^n - 3)/2$	4	$(-\alpha_{04},\alpha_{22})$
	3	$[(3^+,-1),(1^-,0),(7^+,1),(6^-,\alpha_{22})]$	$66\cdot 9^n - 6\cdot 5^n$	4	$(-\alpha_{04},\alpha_{22})$
	4	$[(0^+,-\alpha_{13}),(1^+,\alpha_{22}),(4^+,\alpha_{13}),(5^+,-\alpha_{22})]$	$96\cdot 9^n - 10\cdot 5^n$	6	$(-\alpha_{14},\alpha_{12})$
	5	$[(0^+,-\alpha_{12}),(4^+,\alpha_{12}),(1^-,0),(6^-,0)]$	$75\cdot 9^n - 6\cdot 5^n$	5	$(\alpha_{1,-2},\alpha_{22})$
	6	$[(0^-,-\alpha_{12}),(1^-,0),(3^-,-1),(2^+,0)]$	$15\cdot 9^n$	7	$(-\alpha_{02},\alpha_{12})$
	7	$[(3^+,-1),(7^+,1),(5^-,-\alpha_{22}),(2^-,-\alpha_{22})]$	$45\cdot 9^n - 4\cdot 5^n$	1	$(-\alpha_{14},\alpha_{22})$
	8	$[(4^-,\alpha_{12}),(1^-,0),(6^-,0)]$	$24\cdot 9^n$	0	$(\alpha_{20},0)$
$n \geq 1$ odd	0	$[(4^-,-\alpha_{1,-2}),(1^-,0),(6^-,0),(7^-,\alpha_{10})]$	$3\cdot 9^n$	3	$(\alpha_{2,-2},\alpha_{1,-2})$
	1	$[(4^-,-1),(3^+,-1),(1^-,0),(7^+,-1)]$	$36\cdot 9^n - 4\cdot 5^n$	0	$(-\alpha_{02},\alpha_{22})$
	2	$[(0^+,1),(2^+,\alpha_{12}),(4^+,-1),(6^+,-\alpha_{12})]$	$(177\cdot 9^n - 22\cdot 5^n - 3)/2$	4	$(-\alpha_{04},\alpha_{22})$
	3	$[(0^-,1),(3^+,-1),(5^-,-\alpha_{22}),(7^+,1)]$	$66\cdot 9^n - 6\cdot 5^n$	4	$(-\alpha_{04},\alpha_{22})$
	4	$[(0^+,-\alpha_{13}),(1^+,\alpha_{22}),(4^+,\alpha_{13}),(5^+,-\alpha_{22})]$	$96\cdot 9^n - 10\cdot 5^n$	6	$(-\alpha_{14},\alpha_{12})$
	5	$[(1^-,\alpha_{22}),(6^-,0),(3^+,-1),(7^+,1)]$	$75\cdot 9^n - 6\cdot 5^n$	5	$(\alpha_{30},0)$
	6	$[(0^-,-\alpha_{12}),(1^-,0),(3^-,-1),(6^-,0)]$	$15\cdot 9^n$	7	$(-\alpha_{02},\alpha_{12})$
	7	$[(0^+,-\alpha_{12}),(1^-,0),(6^-,0),(4^+,\alpha_{12})]$	$45\cdot 9^n - 4\cdot 5^n$	1	$(-\alpha_{14},\alpha_{22})$
	8	$[(4^-,\alpha_{12}),(1^-,0),(6^-,0)]$	$24\cdot 9^n$	0	$(\alpha_{20},0)$

Table VIII (c)

EXAMPLE II: RETURN PATHS

n	j	level-$(n-1)$ return path for $D_j^{(n)}$
-1	0	$0, 3, 4, 10, 1, 3, 6, 8, 1, 11, 4, 10, 2, 0$
	1	$0, 3, 4, 10, 1, 3, 6, 8, 1, 11, 4, 9, 4, 10, 1, 3, 6, 8, 1, 11, 4, 8, 0$
	2	$0, 3, 4, 10, 1, 3, 6, 8, 1, 11, 4, 8, 0$
	3	$0, 2, 0$
	4	$0, 2, 11, 4, 10, 3, 5, 7, 8, 11, 4, 10, 2, 0$
	5	$0, 2, 11, 4, 10, 2, 0$
	6	$0, 2, 11, 4, 10, 1, 3, 6, 8, 1, 11, 4, 8, 0$
	7	$0, 2, 1, 0$
	8	$0, 1, 2, 0$
0	0	$7, 7$
	1	$7, 6, 3, 3, 2, 7$
	2	$7, 6, 3, 3, 0, 8, 8, 2, 4, 2, 7$
	3	$7, 6, 3, 3, 0, 8^5, 2, 7$
	4	$7, 6, 3, 3, 1, 3, 3, 0, 8^5, 2, 7$
	5	$7, 3, 3, 8, 8, 2, 3, 3, 0, 8^5, 2, 7$
	6	$7, 3, 3, 8, 8, 3, 7$
	7	$7, 6, 3, 3, 0, 8, 8, 3, 7$
	8	$7, 3, 3, 8^5, 3, 7$
$n \geq 2$ even	0	$8, 0, 8$
	1	$8, 0, 7, 0^4, 5, 0, (6, 0)^2, 1, 0^4, 5, 0, 8$
	2	$8, 0, 7, 0^4, 5, 0, (6, 0)^2, 1, 0^4, 3, 0, 6, 0^4, 6, 0^4, 6, 0, 1, 0^4, 5, 0, 7, 0, 2, 0, 6, 0, 1, 0^4, 5, 0, 8$
	3	$8, 0, 7, 0^4, 5, 0, (6, 0)^2, 1, 0^4, 3, 0, (6, 0^4)^5, 6, 0, 1, 0^4, 5, 0, 8$
	4	$8, 0, 7, 0^4, 5, 0, (6, 0)^2, 1, 0^4, 4, 0^4, 5, 0, (6, 0)^2, 1, 0^4, 3, 0, (6, 0^4)^5, 6, 0, 1, 0^4, 5, 0, 8$
	5	$8, 0, 6, 0, (6, 0^4)^2, 6, 0, 1, 0^4, 5, 0, 6, 0, 6, 0, 1, 0^4, 3, 0, (6, 0^4)^5, 6, 0, 1, 0^4, 5, 0, 8$
	6	$8, 0, 6, 0, (6, 0^4)^2, (6, 0)^2, 8$
	7	$8, 0, 7, 0^4, 5, 0, (6, 0)^2, 1, 0^4, 3, 0, (6, 0^4)^2, (6, 0)^2, 8$
	8	$8, 0, 6, 0, (6, 0^4)^5, (6, 0)^2, 8$
$n \geq 1$ odd	0	$8, 0, 8$
	1	$8, 0, 5, 0^4, 1, 0, (6, 0)^2, 5, 0^4, 7, 0, 8$
	2	$8, 0, 5, 0^4, 1, 0, 6, 0, 2, 0, 7, 0, 5, 0^4, 1, 0, (6, 0^4)^2, 6, 0, 3, 0^4, 1, 0, (6, 0)^2, 5, 0^4, 7, 0, 8$
	3	$8, 0, 5, 0^4, 1, 0, (6, 0^4)^5, 6, 0, 3, 0^4, 1, 0, (6, 0)^2, 5, 0^4, 7, 0, 8$
	4	$8, 0, 5, 0^4, 1, 0, (6, 0^4)^5, 6, 0, 3, 0^4, 1, 0, (6, 0)^2, 5, 0^4, 4, 0^4, 1, 0, (6, 0)^2, 5, 0^4, 7, 0, 8$
	5	$8, 0, 5, 0^4, 1, 0, (6, 0^4)^5, 6, 0, 3, 0^4, 1, 0, (6, 0)^2, 5, 0^4, 1, 0, (6, 0^4)^2, (6, 0)^2, 8$
	6	$8, 0, 6, 0, (6, 0^4)^2, (6, 0)^2, 8$
	7	$8, 0, 6, 0, (6, 0^4)^2, 6, 0, 3, 0^4, 1, 0, (6, 0)^2, 5, 0^4, 7, 0, 8$
	8	$8, 0, 6, 0, (6, 0^4)^5, 6, 0, 6, 0, 8$

TABLE IX

EXAMPLE II: PERIODIC DOMAINS

n	j	domain $\Pi_j^{(n)}$	return time	return path
-1	0	$[(0^-, -\alpha_{12}), (1^-, 0), (2^-, -\alpha_{22}), (3^-, -\alpha_{10})$ $(4^-, -\alpha_{10}), (5^-, -\alpha_{22}), (6^-, 0), (7^-, -\alpha_{12})]$	2	3
	1	$[(0^+, -\alpha_{12}), (1^-, 0), (4^+, \alpha_{12}), (7^-, -\alpha_{12})]$	8	53
$n \geq 0$	0	$[(0^-, \alpha_{10}), (1^-, 0), (2^-, \alpha_{02}), (3^-, -\alpha_{1,-2})$ $(4^-, -\alpha_{1,-2}), (5^-, \alpha_{02}), (6^-, 0), (7^-, \alpha_{10})]$	$3 \cdot 9^n$	0
	1	$[(0^-, -\alpha_{12}), (1^-, 0), (2^-, -\alpha_{22}), (3^-, -\alpha_{10})$ $(4^-, -\alpha_{10}), (5^-, -\alpha_{22}), (6^-, 0), (7^-, -\alpha_{12})]$	$2 \cdot 9^n$	06
	2	$[(0^-, \alpha_{56}), (1^-, 0), (2^-, \alpha_{24}), (3^-, \alpha_{36})$ $(4^-, -\alpha_{10}), (5^-, \alpha_{46}), (6^-, \alpha_{22}), (7^-, \alpha_{10})]$	$3 \cdot 9^n$	00060
$n \geq 0$ even	3	$[(3^+, -\alpha_{10}), (0^-, -\alpha_{24}), (7^+, \alpha_{10}), (4^-, -\alpha_{10})]$	$84 \cdot 9^n - 4 \cdot 5^n$	706060
$n \geq 1$ odd	3	$[(0^+, -\alpha_{12}), (1^-, 0), (4^+, \alpha_{12}), (5^-, -\alpha_{34})]$	$84 \cdot 9^n - 4 \cdot 5^n$	706060

Table X (a)

EXAMPLE II: PARTITION OF BASELINE

n	ζ^*	$j^{(n)}$	$j^{(n+1)}$	coordinates	length	t_j	$\tilde{t}_j$
Ω	$(0,0)$	10	—	$(-\tau,\tau)$	—	—	—
			0	—	$-2-3\tau$	3	3
			1	$(-\tau,-2-2\tau)$	0	3	3
			2	—	$3+4\tau$	3	3
			1	$(-\tau,1+2\tau)$	0	13	5
			6	—	$-2-3\tau$	4	4
			4	$(-\tau,-1-\tau)$	0	4	4
			5	—	$3+4\tau$	4	4
			4	$(-\tau,2+3\tau)$	0	11	3
			0	—	$-2-3\tau$	11	3
		9	1	$(-\tau,0)$	0	11	3
		8	2	—	$3+4\tau$	11	3
			1	$(-\tau,3+4\tau)$	0	21	7
			6	—	$-2-3\tau$	12	4
			4	$(-\tau,1+\tau)$	0	8	0
			6	—	$-2-3\tau$	8	0
			1	$(-\tau,-1-2\tau)$	0	17	1
			2	—	$3+4\tau$	7	7
			1	$(-\tau,2+2\tau)$	0	7	7
			0	—	$-2-3\tau$	7	7
		7	4	$(-\tau,-\tau)$	0	7	7
-1	$(-1-\tau,\ \tau)$	2	—	$(-\tau,0)$	—	—	—
			5	—	$5+7\tau$	5	5
			2	$(5+6\tau,-7-10\tau$	0	7	7
			5	—	$5+7\tau$	14	1
			4	$(10+13\tau,-14-20\tau)$	0	13	2
			3	—	$-12-17\tau$	10	0
			2	$(-2-4\tau,3+4\tau)$	0	9	0
			1	—	$5+7\tau$	4	4
		1	4	$(3+3\tau,-4-6\tau)$	0	4	4
		0	7	—	$5+7\tau$	4	4
			2	$(8+10\tau,-11-16\tau)$	0	4	4
			3	—	$-12-17\tau$	4	4
			4	$(-4-7\tau,6+8\tau)$	0	7	6
			5	—	$5+7\tau$	8	5
			—	$(1,-1-2\tau)$	—	—	—
		5	—	$(-1-2\tau,0)$	—	—	—
			$\Pi_1^{(-1)}$	—	$3+4\tau$	—	—
		4	2	$(-1-2\tau,3+4\tau)$	0	8	3
		6	1	—	$5+7\tau$	1	3
			4	$(-1-2\tau,8+11\tau)$	0	1	3
			7	—	$5+7\tau$	1	3
			2	$(-1-2\tau,13+18\tau)$	0	1	3
			3	—	$-12-17\tau$	1	3
			—	$(-1-2\tau,1+\tau)$	—	—	—

Table X (b)

EXAMPLE II: PARTITION OF BASELINE

n	ζ^*	$j^{(n)}$	$j^{(n+1)}$	coordinates	length	t_j	$\tilde{t}_j$
$n \geq 0$ even	$(-1-\tau, \tau)$	3	—	$(-\alpha_{0,1}, 0)$	—	—	—
			7	—	$\alpha_{5,7}$	16	5
			2	$(\alpha_{56}, -\alpha_{7,10})$	0	34	0
			3	—	$-\alpha_{12,17}$	36	0
			4	$(-\alpha_{7,11}, \alpha_{10,14})$	0	36	0
			5	—	$\alpha_{5,7}$	36	0
		2	2	$(-\alpha_{24}, \alpha_{34})$	0	11	1
		7	$\Pi_3^{(n)}$	—	α_{34}		
			2	$(\alpha_{10}, -\alpha_{12})$	0	13	0
			1	—	α_{57}	18	4
			4	$(\alpha_{67}, -\alpha_{8,12})$	0	68	2
			7	—	α_{57}	32	5
			2	$(\alpha_{11,14}, -\alpha_{15,22})$	0	50	0
			3	—	$-\alpha_{12,17}$	52	0
		4	4	$(-\alpha_{13}, \alpha_{22})$	0	52	0
		1	5	—	α_{57}	52	0
			2	$(\alpha_{44}, -\alpha_{58})$	0	20	5
			5	—	α_{57}	7	4
			4	$(\alpha_{9,11}, -\alpha_{12,18})$	0	7	4
			3	—	$-\alpha_{12,17}$	7	4
			2	$(-\alpha_{36}, \alpha_{56})$	0	7	4
			1	—	α_{57}	7	4
			4	$(\alpha_{21}, -\alpha_{24})$	0	57	2
			7	—	α_{57}	21	5
			2	$(\alpha_{78}, -\alpha_{9,14})$	0	39	0
			3	—	$-\alpha_{12,17}$	41	0
			4	$(-\alpha_{59}, \alpha_{8,10})$	0	41	0
			5	—	α_{57}	41	0
		5	—	$(-\alpha_{12}, 0)$	—	—	—
			1	—	α_{57}	13	3
			4	$(-\alpha_{12}, \alpha_{57})$	0	63	1
			7	—	α_{57}	27	4
			2	$(-\alpha_{12}, \alpha_{10,14})$	0	45	7
			3	—	$-\alpha_{12,17}$	47	7
			4	$(-\alpha_{12}, -\alpha_{23})$	0	47	7
			5	—	α_{57}	47	7
			2	$(-\alpha_{12}, \alpha_{34})$	0	15	4
			5	—	α_{57}	2	3
			4	$(-\alpha_{12}, \alpha_{8,11})$	0	2	3
			3	—	$-\alpha_{12,17}$	2	3
			2	$(-\alpha_{12}, -\alpha_{46})$	0	2	3
			1	—	α_{57}	2	3
			—	$(-\alpha_{12}, \alpha_{11})$	—	—	—

Table X (c)

EXAMPLE II: PARTITION OF BASELINE

n	ζ^*	$j^{(n)}$	$j^{(n+1)}$	coordinates	length	t_j	$\tilde{t}_j$
$n \geq 1$ odd	$(-1-\tau, \tau)$	1	—	$(-\alpha_{0,1}, 0)$	—	—	—
			5	—	α_{57}	16	5
			2	$(\alpha_{56}, -\alpha_{7,10})$	0	32	7
			5	—	α_{57}	61	1
			4	$(\alpha_{10,13}, -\alpha_{14,20})$	0	63	2
			3	—	$-\alpha_{12,17}$	47	4
			2	$(-\alpha_{21}, \alpha_{34})$	0	45	0
			1	—	α_{57}	13	4
			4	$(\alpha_{33}, -\alpha_{46})$	0	13	4
			7	—	α_{57}	13	4
			2	$(\alpha_{8,10}, -\alpha_{11,16})$	0	13	4
			3	—	$-\alpha_{12,17}$	13	4
			4	$(-\alpha_{47}, \alpha_{68})$	0	29	6
			5	—	α_{57}	27	5
		2	2	$(-\alpha_{1,0}, -\alpha_{12})$	0	41	7
		3	5	—	α_{57}	32	1
			4	$(\alpha_{67}, -\alpha_{8,12})$	0	34	2
			3	—	$-\alpha_{12,17}$	18	0
			2	$(-\alpha_{6,10}, \alpha_{9,12})$	0	18	0
			7	—	α_{57}	18	0
		4	4	$(-\alpha_{13}, \alpha_{22})$	0	18	0
		5	1	—	α_{57}	18	0
			2	$(\alpha_{44}, -\alpha_{58})$	0	50	4
			3	—	$-\alpha_{12,17}$	52	0
			4	$(-\alpha_{8,13}, \alpha_{12,16})$	0	68	6
			5	—	α_{57}	66	5
			2	$(-\alpha_{36}, \alpha_{56})$	0	37	3
			5	—	α_{57}	21	1
			4	$(\alpha_{21}, -\alpha_{24})$	0	23	2
			3	—	$-\alpha_{12,17}$	7	0
			2	$(-\alpha_{10,16}, \alpha_{15,20})$	0	7	0
			7	—	α_{57}	7	0
			4	$(-\alpha_{59}, \alpha_{8,10})$	0	7	0
			1	—	α_{57}	7	0
			—	$(-\alpha_{02}, \alpha_{10})$	—	—	—
		7	—	$(-\alpha_{12}, 0)$	—	—	—
			$\Pi_3^{(n)}$	—	α_{34}	—	—
			2	$(-\alpha_{12}, \alpha_{34})$	0	39	3
			1	—	α_{57}	2	3
			4	$(-\alpha_{12}, \alpha_{8,11})$	0	2	3
			7	—	α_{57}	2	3
			2	$(-\alpha_{12}, \alpha_{13,18})$	0	2	3
			3	—	$-\alpha_{12,17}$	2	3
			—	$(-\alpha_{12}, \alpha_{11})$	—	—	—

References

[1] R. Adler, B. Kitchens and C. Tresser, Dynamics of nonergodic piecewise affine maps of the torus, *Ergod. Th. and Dynam. Sys.* **21** (2001) 959–999.

[2] T. M. Apostol, Introduction to analytic number theory, Springer Verlag, (1976).

[3] P. Ashwin, Elliptic behaviour in the sawtooth standard map, *Phys. Lett. A* **232** (1997) 409–416.

[4] P. Ashwin, W. Chambers, and G. Petrov, Lossless digital filters overflow oscillations: approximations of invariant fractals, *Inter. J. Bifur. Chaos*, **7** (1997) 2603–2610.

[5] D. Bosio and F. Vivaldi, Round-off errors and p-adic numbers, *Nonlinearity* **13** (2000) 309–322.

[6] J. Buzzi, Piecewise isometries have zero topological entropy, Dynamics of nonergodic piecewise affine maps of the torus, *Ergod. Th. and Dynam. Sys.* **21** (2001) 1371–1377.

[7] L. O. Chua and T. Lin, Chaos in digital filters, *IEEE Trans. Circuits and Systems,* **CAS-35** (1988) 648–658.

[8] L. O. Chua and T. Lin, Chaos and fractals from third order digital filters, *Int. J. Cir. Theor. Appl.* **18** (1990) 241–255.

[9] L. O. Chua and T. Lin, Fractal pattern of second order non-linear digital filters: a new symbolic analysis, *Int. J. Cir. Theor. Appl.* **18** (1990) 541–550.

[10] H. Cohn, *Advanced number theory*, Dover, New York, 1980

[11] A. C. Davies, Nonlinear oscillations and chaos from digital filters overflow, *Phil. Trans. R. Soc. Lond.* **A 353** (1995) 85–99.

[12] A. Goetz, Sofic subshifts and piecewise isometric systems, *Ergod. Theor. & Dyn. Sys.* **19** (1999) 1485–1501.

[13] A. Goetz, Dynamics of piecewise isometries, *Illinois Journal of Mathematics* **44** (2000) 465–478.

[14] A. Goetz, Stability of piecewise rotations and affine maps, *Nonlinearity* **14** (2001) 205–219.

[15] E. Gutkin and N. Simanyi, Dual polygonal billiards and necklage dynamics, *Comm. Math. Phys* **143** (1992) 431–449.

[16] E. Gutkin and N. Haydn, Topological entropy of polygon exchange transformations and polygonal billiards, *Ergod. Th. and Dyn. Sys.* **17** (1997) 849–867.

[17] G. H. Hardy and E. M. Wright, *An introduction to the theory of numbers*, Oxford University Press, Oxford, (1979).

[18] B. Khang, Dynamics of symplectic affine maps on tori, PhD Thesis, University of Illinois at Urbana-Champain (2000).

[19] J. H. Lowenstein, S. Hatjispyros and F. Vivaldi, Quasi-periodicity, global stability and scaling in a model of Hamiltonian round-off, *Chaos* **7** (1997) 49–66.

[20] J. H. Lowenstein and F. Vivaldi, Anomalous transport in a model of hamiltonian round-off errors, *Nonlinearity* **11** (1998) 1321–1350

[21] J. H. Lowenstein and F. Vivaldi, Embedding dynamics for round-off errors near a periodic orbit, *Chaos* **10** (2000) 747-755.

[22] S. Tabachnikov, Dual billiards, *Russian Math. Surveys*, **48** (1993) 81–109.

[23] F. Vivaldi and A. V. Shaidenko, Global stability of a class of discontinuous dual billiards, *Commun. Math. Phys.*, **110** (1987) 625–640.

[24] F. Vivaldi and I. Vladimirov, Pseudo-randomness of round-off errors in discretized linear maps on the plane, preprint, Queen Mary, University of London (2001) `http://www.ma.utexas.edu/mp_arc-bin/mpa?yn=01-149`.

[25] C. W. Wu and L. O. Chua, Properties of admissible sequences in a second-order digital filter with overflow non-linearity, *Int. J. Cir. Theoer. Appl.* **21** (1993) 299–307.

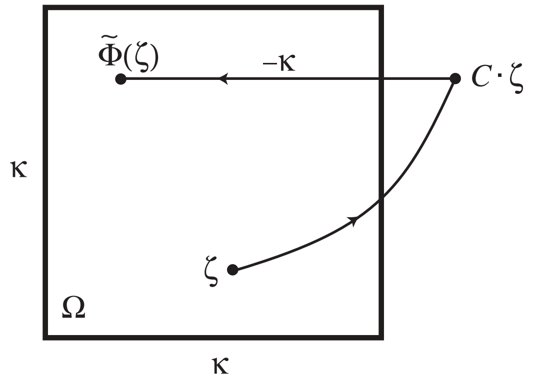

Figure 1: Action of the torus map Φ. To obtain $\Phi(\zeta)$ for arbitrary $\zeta \in \Omega$, we rotate it to $C \cdot \zeta$ and then map it back to Ω with a suitable (and unique) lattice translation.

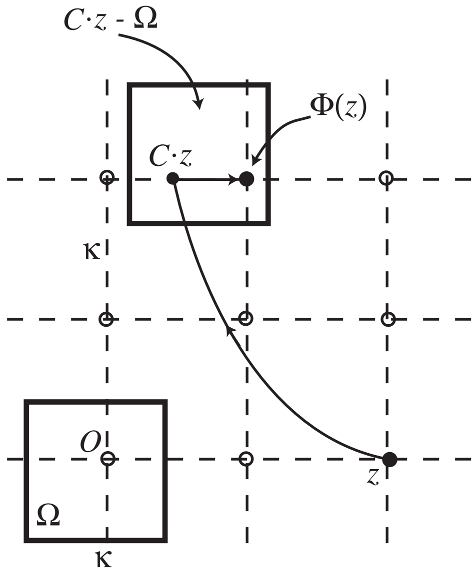

Figure 2: Action of the lattice map Ψ. To obtain $\Psi(z)$ for arbitrary $z \in \mathbf{Z}^2$, we rotate it to $C \cdot z$ and then map to the unique lattice point in the square $C \cdot z - \Omega$. The precise nature of the rounding process depends on the position of the square relative to the origin.

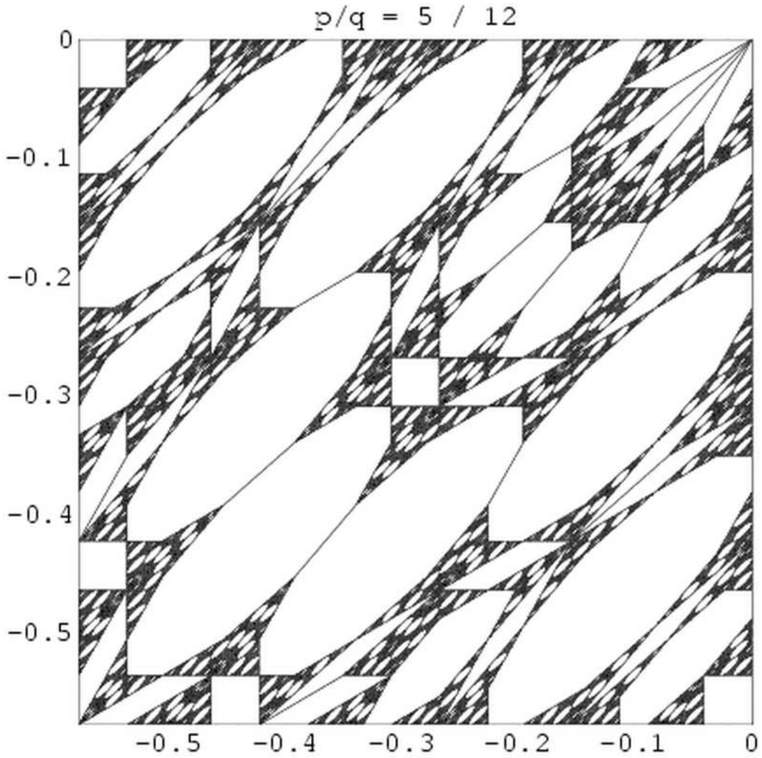

Figure 3: The discontinuity set of the map Φ for the rotation number $p/q = 5/12$.

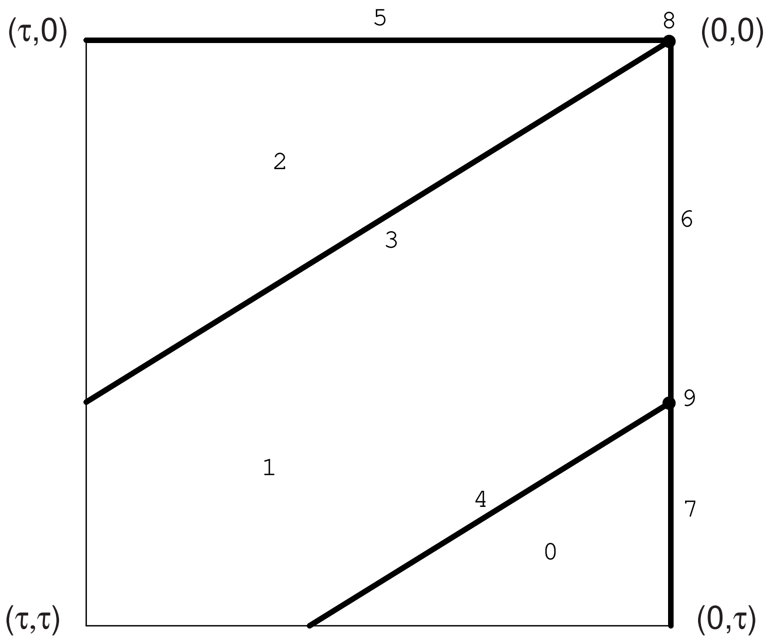

Figure 4: Example I: generating partition. The domains $0, 1, 2$ are open polygons; 3 to 7 are open line segments; 8, 9 are points. Each domain is assigned return time 1. The action of the map on each domain D is affine: $\Phi(D) = \tilde{C}D + \delta$, with δ depending on the domain.

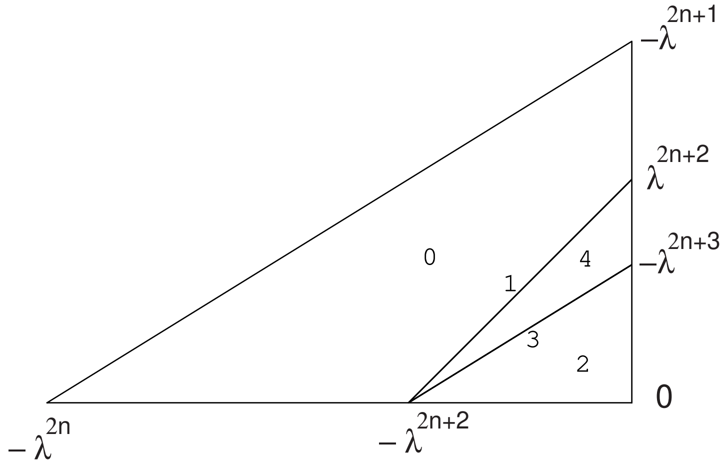

Figure 5: Example I: level-n return map partition. All coordinates are relative to the accumulation point at $(0,\, \tau)$. The domains $0, 2, 4$ are open polygons; $1, 3$ are open segments.

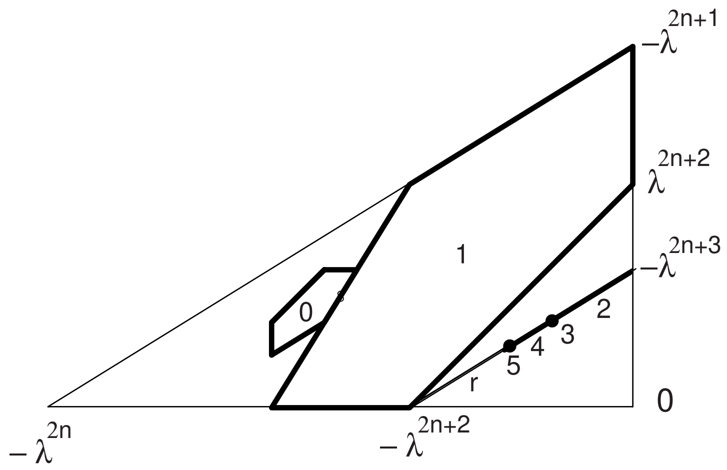

Figure 6: Example I: periodic domains, $\Pi_j^{(n)}$, for $n \geq 0$. The labels represent the values of j. The domains 0 and 1 are open polygons; 2 and 4 are open line segments; 3 and 5 are points. The segment r in domain $D_3^{(n)}$ is the image of $D_3^{(n+1)}$, under iterated application of the level-n return map. This diagram thus gives a recursive picture of the complete periodic-orbit structure of $D_3^{(n)}$. Note the following ratios of lengths: $|2| : |4| : |r| : |D_3^{(n)}| = \lambda^2 : |\lambda|^3 : \lambda^2 : 1$.

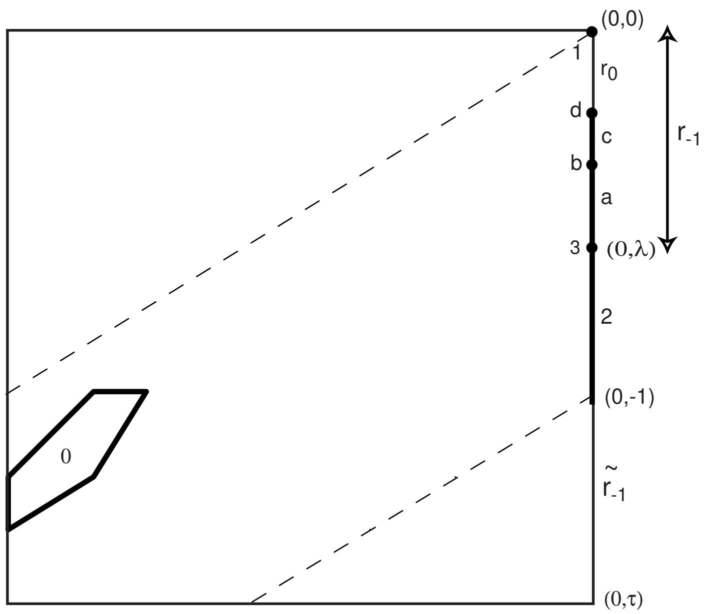

Figure 7: Example I: periodic domains of level -1. 0 is an open pentagon; 2, a and c are open line segments; 3, b, and d are points. The point $(0,-1)$ lies on the same period-7 orbit as 6. The interval r_{-1} is mapped into its mirror image $\tilde{r_{-1}}$ by five iterations of the dynamical map.

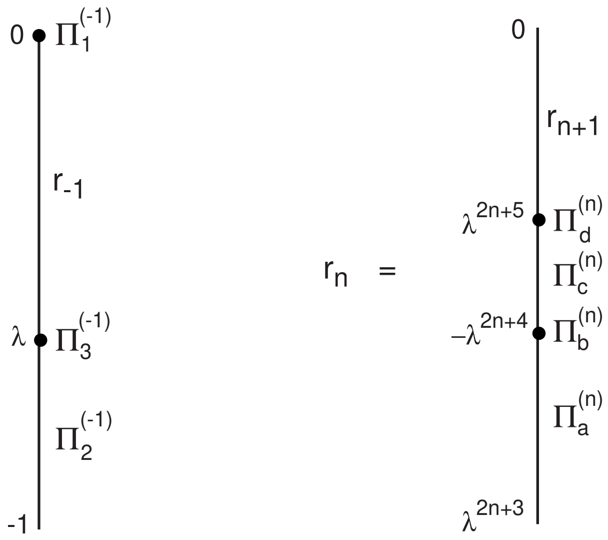

Figure 8: Periodic-orbit decomposistion of the discontinuity set baseline $\mathcal{B}$ (recursive form).

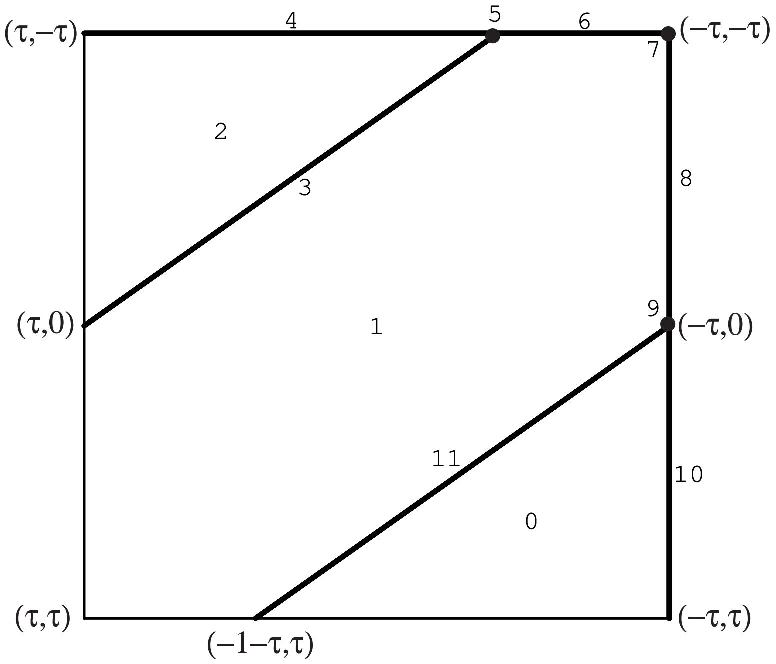

Figure 9: Example II: generating partition. The domains $0, 1, 2$ are open polygons; $3, 4, 6, 8, 10, 11$ are open line segments; $5, 7, 9$ are points. Each domain is assigned return time 1.

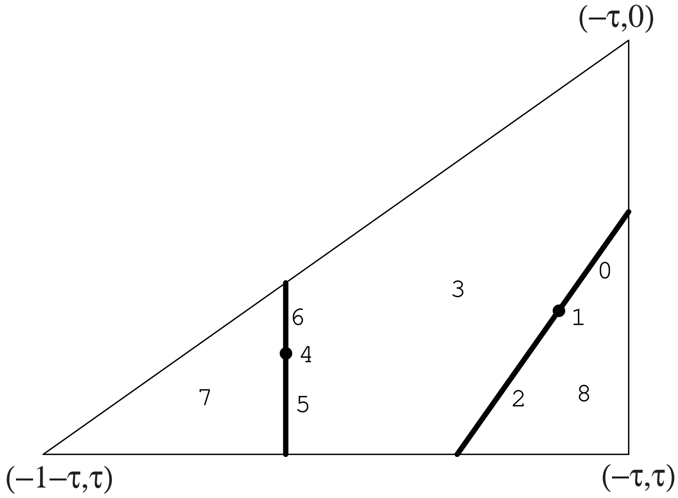

Figure 10: Example II: level-(-1) return map partition. The domains 3, 7, 8 are open polygons; $0, 2, 5, 6$ are open line segments; $1, 4$ are points.

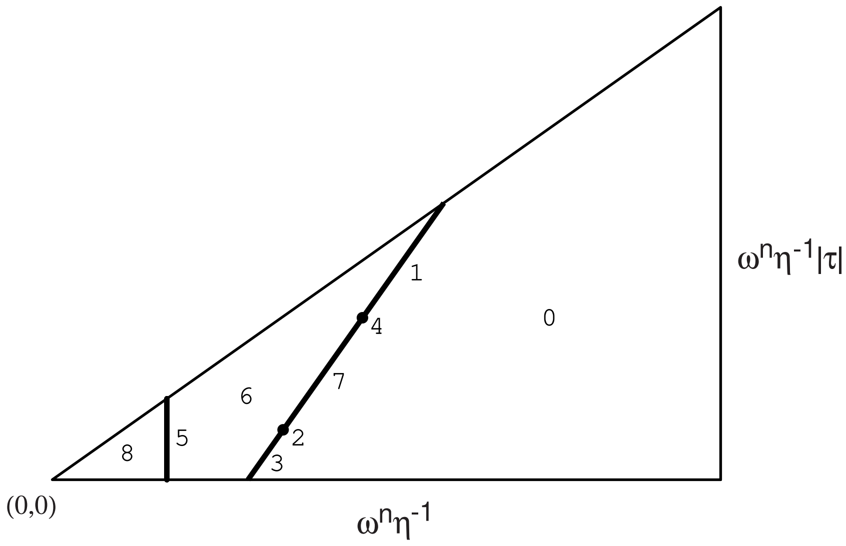

Figure 11: Example II: level-n return map partition, $n = 0, 2, 4, 6, \ldots$. The domains 0, 6, 8 are open polygons; $1, 3, 5, 7$ are open line segments; $2, 4$ are points.

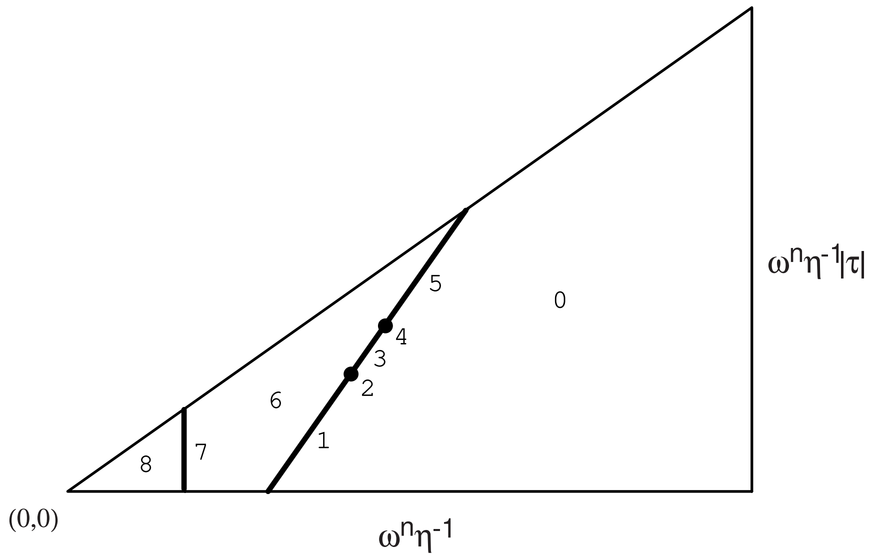

Figure 12: Example II: level-n return map partition, $n = 1, 3, 5, 7, \ldots$. The domains 0, 6, 8 are open polygons; $1, 3, 5, 7$ are open line segments; $2, 4$ are points.